2019-06-07

Exploring mechanisms for spring bloom evolution: contrasting 2008 and 2012 blooms in the southwest Pacific Ocean

Chiswell, SM

10.1093/plankt/fbz017
Journal of Plankton Research
Oxford University Press (OUP)

EXPLORING MECHANISMS FOR SPRING BLOOM EVOLUTION: CONTRASTING 2008 AND 2012 BLOOMS IN THE SOUTH WEST PACIFIC OCEAN

STEPHEN M. CHISWELL [1]
KARL SAFI [2]
SYLVIA G. SANDER [3,7]
ROBERT STRZEPEK[4]
MICHAEL J. ELLWOOD[5]
ANGELA MILNE[6]
PHILIP W. BOYD [2,4]

[1] National Institute of Water and Atmospheric Research, PO Box 14-901, Wellington, New Zealand

[2] National Institute of Water and Atmospheric Research, PO Box 11-115, Hamilton, New Zealand

[3] Department of Chemistry, NIWA/University of Otago Research Centre for Oceanography, University of Otago, Dunedin, New Zealand

[4] Institute for Marine and Antarctic Studies, University of Tasmania, Hobart, Australia

[5] Research School of Earth Sciences, Australian National University, Canberra, Australia

[6] School of Geography, Earth and Environmental Sciences, University of Plymouth, Plymouth PL4 8AA, United Kingdom

[7] Marine Environmental Studies Laboratory, IAEA Environment Laboratories, Department of Nuclear Science and Applications, International Atomic Energy Agency, Monaco, Principality of Monaco

CORRESPONDING AUTHOR: s.chiswell@niwa.cri.nz

Abstract

Observations from two research cruises made in 2008 and 2012 to east of New Zealand are put into context with satellite data to contrast and compare surface chlorophyll *a* evolution in the two years in order to explore mechanisms of phytoplankton bloom development in the southwest Pacific Ocean.

In 2008, sea surface chlorophyll *a* largely followed the long-term climatological cycle, and 2008 can be considered a canonical year, where the autumn bloom is triggered by increasing vertical mixing at the end of summer, and the spring bloom is triggered by decreasing vertical mixing at the end of winter. In contrast, 2012 was anomalous in that there was no autumn bloom, and in early spring there were several periods of sustained increase in surface chlorophyll *a* that did not become fully developed spring blooms. (In this region, we consider spring blooms to occur when surface chlorophyll *a* exceeds 0.5 mg m^{-3}). These events can be related to alternating episodes of increased or decreased vertical mixing. The eventual spring bloom in October was driven by increased ocean cooling and wind stress and, paradoxically, was driven by mechanisms considered more appropriate for autumn rather than spring blooms.

Keywords Primary production, spring bloom, physical control, wind mixing, heat flux

INTRODUCTION

Spring blooms of phytoplankton are a near-global phenomenon in subtropical, temperate and subpolar oceans (e.g., Cole *et al.*, 2015, Westberry *et al.*, 2016). Perhaps the most prominent and most studied spring bloom is in the North Atlantic Ocean, (e.g., Henson *et al.*, 2009, and references therein). However, spring blooms have also been observed in the southwest Pacific Ocean, although surface chlorophyll levels there are considerably less than in the North Atlantic Ocean and may only reach 1 mg m^{-3} (Chiswell *et al.*, 2013).

There are several theories for the cause and timing of spring blooms, and many are one-dimensional (1-d) in the vertical based around some mechanism that retains phytoplankton in the photic zone near the surface in the spring.

A commonly cited hypothesis, referred to here as the shoaling mixed layer hypothesis (SMLH), is based on Sverdrup (1953). Under the SMLH, the spring bloom is considered to start when the mixed layer shoals to be less than the critical depth (e.g., Dutkiewicz *et al.*, 2001, Levy, 2015). However, observations of spring blooms occurring before the mixed layer began to shoal led to hypotheses that blooms are initiated by the shutdown of turbulent mixing (Huisman *et al.*, 1999, Taylor & Ferrari, 2011) or by the onset of near-surface stratification (Chiswell, 2011).

These theories appear to be contradictory, but Chiswell *et al.* (2015b) showed that much of the contradiction disappears when one is careful to distinguish between surface phytoplankton concentrations and depth-integrated phytoplankton stock. Chiswell *et al.* (2015b) proposed a 1-d model, where there is a transition from deep winter mixing to a well-mixed but low turbulence regime in early spring, and then another transition to a (density) stratified regime later in the spring once surface waters begin to warm. In their model, Chiswell *et al.* (2015b) suggested that after an autumn bloom, surface phytoplankton concentrations decrease during deep winter mixing due to dilution (e.g., Evans & Parslow, 1985) and may start to increase once the low-turbulence regime commences (e.g., Huisman *et al.*, 1999, Taylor & Ferrari, 2011), but it is only when the ocean begins to stratify that surface production is maximised. Chiswell *et al.* (2015b) note that the depth-integrated phytoplankton stock shows quite different behaviour than surface phytoplankton concentration. Depth-integrated phytoplankton stock can either decrease during winter if winter mixing is deep compared to the photic zone (typically at higher latitudes), or can increase

during winter if winter mixing is shallow compared to the photic zone (typically lower latitudes).

Many of the arguments supporting the various spring bloom hypotheses and the unified interpretation by Chiswell *et al.* (2015b), are based on observed correlations between various bloom metrics and forcing quantities. For example, between mixed layer depth (MLD) and chlorophyll concentration (Henson *et al.*, 2006), between bloom initiation and the end of convective forcing (Taylor & Ferrari, 2011), between bloom initiation and the net heat flux (NHF) sign change (Cole *et al.*, 2015), or between the seasonal progression of the spring bloom and the seasonal progression of the wind stress (Chiswell *et al.*, 2013).

However, there is a danger in inferring a causal connection from the correlation of quantities (i.e., NHF, MLD and wind stress) that are inherently driven by the same solar insolation, and so the relative roles of NHF, MLD and wind stress in the timing of spring blooms are still open to some debate.

Here, to further explore the mechanisms of bloom development, we compare the time evolution of blooms in Subtropical Waters east of New Zealand. In both 2008 and 2012, research cruises were made to the same region east of the North Island (Figure 1) during the spring with the aim of describing bloom development. During each cruise, measurements of size-fractionated primary production and biomass, nutrients, NHF, MLD and other quantities were made following a floating array deployed near the centre of an anticyclonic mesoscale eddy.

Data from the 2008 cruise have been analysed by Chiswell (2011), and were the basis for the onset of stratification hypothesis. Here, we start with a similar analysis of the 2012 data. After this comparison, we use satellite data to put the cruise observations into context of their respective years. In 2008, sea surface chlorophyll concentration largely followed the long-term climatological cycle and 2008 can be considered a canonical year. In contrast, in 2012 was anomalous in that there was no autumn bloom, and in winter and spring there were events that did not become fully developed spring blooms. We consider the departures from climatology in each year to explain these events. We then address the question of how representative the experimental site is of the region in general by considering surface chlorophyll in the

region derived from satellite. Finally, we discuss our results and present our conclusions.

Before proceeding further, it is worth commenting on the use of the term 'bloom'. There have been various definitions of a spring bloom. These definitions often include a threshold, for example when surface chlorophyll exceeds 1 mg m^{-3} (e.g., Brody *et al.*, 2013), although as Smayda (1997) notes, what constitutes a bloom may have regional and species-specific aspects. Here we use the term 'spring bloom' when surface chlorophyll exceeds 0.5 mg m^{-3} to reflect the observations that spring blooms are weaker in the southwest Pacific Ocean than in the Atlantic Ocean. An 'autumn bloom' is defined by a threshold level of 0.25 mg m^{-3}.

METHODS

Shipboard measurements

Hydrography

Cruises were made in both 2008 and 2012 to the same location east of the North Island (Figure 1). These cruises were part of an iron cycling project, and are known as FeCycle II and FeCycle III, respectively. Data from the 2008 cruise (FeCycle II) have been reported elsewhere (Chiswell, 2011, Twining *et al.*, 2014).

Each cruise lasted from mid-September until early October. Prior to each cruise, satellite altimeter data were scanned to choose an anti-cyclonic mesoscale eddy close to the nominal study site. Upon arrival at the site, a shipboard ADCP survey was made of the eddy, then a Lagrangian floating array extending to ~120 m was deployed in the eddy centre.

During each cruise, daily CTD casts were made at 3 am and noon close to the Lagrangian array. In 2012, the array was lost toward the end of the cruise, after which casts were made at the estimated eddy centre. CTD casts were also made at other times of the day, not necessarily near the Lagrangian array, for a variety of different experiments. To avoid issues associated with non-photochemical quenching (e.g., Müller *et al.*, 2001) the primary data used here are the 3 am casts.

Water samples for chlorophyll, phytoplankton and microzooplankton and nutrient analyses were collected on upcasts using 24 10-L Niskin bottles mounted on the CTD rosette.

For each CTD cast, two estimates of the mixed layer depth (MLD_1 and MLD_2) were computed as the depths where the *in situ* density exceeded the surface value by 0.125 and 0.025 kg m^{-3}, respectively (Chiswell, 2011, Chiswell *et al.*, 2013). In this region, MLD_1 can be considered the depth of the seasonal thermocline, whereas MLD_2 reflects weak stratification that would normally be considered to be within the mixed layer (Chiswell, 2011).

Meteorology

Continuous surface measurements of 10-m wind speed, sea surface temperature, sea surface salinity and sea surface transmissivity were also made from the ship's underway sampling system. Surface stress was calculated from 10-m wind speed, W, as $\tau = \rho_a c_d W^2$, where the air density, ρ_a, was set to 1 kg m^{-3}, and the drag coefficient, c_d was set to 1.5×10^{-3} (e.g., Kara *et al.*, 2007).

In 2012, sensible and latent heat fluxes were calculated from ship-based measurements of wind speed, atmospheric pressure, humidity, irradiance and air and sea surface temperature using the bulk formulae of the NOAA COARE3.1 algorithms (Fairall *et al.*, 2011).

Nutrients

Macronutrients from the upcast water samples were determined using an automated micro-segmented flow analyser with digital detector (Pickmere, 1998). Dissolved iron (dFe) was measured at a set of predetermined depths using standard trace-metal sampling (i.e., a trace-metal clean rosette and Kevlar line), and was determined using flow injection analysis (Floor *et al.*, 2015, Obata *et al.*, 2002). Further analytical details are described in Chandrasekhar *et al.* (2018).

Chlorophyll

The CTD fluorometer was calibrated against chlorophyll obtained from 500 mL samples taken from each water bottle on the CTD casts. Chlorophyll extractions were performed following Parsons *et al.* (1984), using acetone extraction. Chlorophyll in

the extracts was determined with a fluorometer calibrated against a pure chlorophyll a standard (Sigma Chemicals).

Size-fractionated primary production

Net primary production was based on radioisotope measurements and 24-hour incubations (e.g., Laws, 1991). Samples were collected pre-dawn from trace-metal clean Niskin bottles deployed on a trace-metal rosette. Water was sampled from three depths: 20, 40, and at one depth within the 60-90 m stratum determined from the previous midday irradiance profiles. Samples were spiked with 20 µCi of Sodium ^{14}C-bicarbonate ($NaH^{14}CO_3$; specific activity 1.85 GBq mmol^{-1}) and then incubated for 24 hours in neutral-density mesh bags in a deckboard incubator at 6 intensities: 80, 50, 30, 15, 3, and 0.5 % of incident irradiance (% I_o) (2008), and 65, 50, 35, 16, 2, and 1 % I_o (2012). These light levels corresponded to *in situ* depths of 2-70 m (2008), and 4-94 m (2012).

Upon completion of the 24-hour incubation, samples were analysed by liquid scintillation counting (Beckman LS 5000).

Phytoplankton and microzooplankton identification and enumeration

For the 2012 cruise, phytoplankton >2 µm and microzooplankton were identified and enumerated in 250 mL subsamples preserved with Lugol's Iodine solution (1% final concentration) using a Leica DMI3000B inverted microscopic. Samples were then counted and identified with an inverted microscope at 100x to 600x magnification.

Phytoplankton were identified where practical to genus or species level but there was no differentiation of plastidic ciliates. Ciliate biomass was estimated from dimensions of 10-20 randomly chosen individuals of each taxon. The volumes were estimated from approximate geometric shapes and were converted to carbon biomass using a factor of 0.19 pg C µm^{-3} (e.g., Putt & Stoecker, 1989). Separate picophytoplankton (<2 µm) samples were frozen in liquid nitrogen (e.g., Lebaron *et al.*, 1998) and thawed immediately before counting by flow cytometry following the methods of Hall and Safi (2001).

In 2008, the diatom species were analysed by using a combination of light microscopy and the abundance of Asterionellopsis16S rDNA sequences as a

195 proportion of diatom sequences, and all photoautotrophic sequences (e.g., Twining *et*
196 *al.*, 2014).

197 ***Satellite estimates of sea surface chlorophyll and temperature***

198 The Moderate Resolution Imaging Spectroradiometer (MODIS, Esaias *et al.*,
199 1998), launched in 2002 provides estimates of sea surface chlorophyll concentration.
200 Data used here are 9-km 8-day composites of sea surface chlorophyll downloaded
201 from NASA, http://oceandata.sci.gsfc.nasa.gov/MODISA/Mapped/8Day/9km/chlor/.

202 These data were composited for 100 km diameter around the nominal cruise
203 location (180°E, 39°S) to provide time series of surface chlorophyll concentration.
204 The climatological annual cycle of surface chlorophyll concentration at the nominal
205 experimental site was computed using the 8-d composite data from 2003 to 2012, and
206 interpolated to daily values.

207 Sea surface temperature (SST) from the Advanced Very-High-Resolution
208 Radiometer (AVHRR) instruments is available from an objectively-analysed product
209 provided by NOAA (NOAA OI SST V2 High Resolution Dataset, Reynolds *et al.*,
210 2007). Here we use the AVHRR only product (https://www.ncdc.noaa.gov/oisst). The
211 climatological annual cycle of SST was computed for the time period 1985 to 2012.

212 ***NCEP surface fluxes***

213 Daily values of wind stress, latent and sensible heat, and long- and short-wave
214 radiation daily fluxes at ~2º resolution were downloaded from the National Centers
215 for Environmental Prediction (NCEP) reanalysis products
216 http://www.esrl.noaa.gov/psd/data/gridded/data.ncep.reanalysis.surfaceflux.html. To
217 be consistent with the MODIS data, annual cycles of these variables at the nominal
218 experimental site were computed using data from 2003 to 2012.

219 ***Argo profiles***

220 The Argo program maintains about 3000 profiling floats around the planet
221 (Gould & Turton, 2006) which provide profiles of temperature and salinity between

2000 m and the surface about every 10 d. Argo data are available from the French Research Institute for Exploitation of the Sea (Ifremer) via their website ftp://ftp.ifremer.fr/ifremer/argo/.

We selected profiles taken within 125 km of the nominal experimental site in each year. This radius was chosen as a compromise between having too few profiles and having profiles that do not reflect the water mass characteristics of the experimental site. There were 42 profiles in 2008, and 23 profiles in 2012 that were within 125 km of the experimental site (Figure 1).

Mixed layer depths MLD_1 and MLD_2 were computed from the temperature and salinity profiles using the same criteria as used to compute mixed layer depth from the CTD.

RESULTS

2008 and 2012 cruise observations

The study area is in a region of Subtropical Water (Chiswell *et al.*, 2015a) where the mean surface chlorophyll derived from MODIS is ~0.3 mg m^{-3} (Figure 1).

Locations of all CTD casts made during the two cruises are shown in Figure 2. In 2008, the Lagrangian array remained close to the centre of the eddy until about 4 days from the end of the experiment, when ship-board Acoustic Doppler Profiler (ADCP) data indicated that the array spun out of the eddy (Chiswell, 2011). In 2012, the array travelled north west with a mean speed of 0.056 m s^{-1}, but showed a looping structure, which suggests that, as in 2008, it was slipping out from the centre. The 3 am and noon CTD casts were made close to the array until 1 October when the array was lost. After this, the eddy centre was estimated from the daily ADCP surveys.

Figure 3 summarises the 3 am data for both cruises, showing temperature and chlorophyll derived from the CTD casts, along with wind stress derived from the ship's anemometer, and two estimates of the mixed layer depth, MLD_1 and MLD_2 (based on density differences of 0.125 and 0.025 kg m^{-3}, see Methods).

The evolution of the MLD and the biological responses during the 2008 cruise (Figure 3, left-hand panels) have been discussed by Chiswell (2011). On arrival at the site, the water column was weakly stratified and near-surface chlorophyll

concentration, C_0, was about 1 mg m^{-3}. Soon after arrival, increasing winds destroyed the stratification and mixed the phytoplankton down, leading to a decrease in C_0. Winds then decreased and an increase in C_0 occurred in the re-emerging stratification. The depth-integrated chlorophyll stock over the upper 300 m, $C_{0/300} = \int_0^{300} C(z)dz$, showed little change during the cruise having a mean ± standard deviation of ~31.2 ± 6.7 mg m^{-2}. There was no significant correlation (r^2= 0.03) between $C_{0/300}$ and C_0 .

Chiswell (2011) interpreted the 2008 data to suggest that spring blooms in surface chlorophyll initiate with the onset of shallow weak stratification that forms during periods of low winds, and that chlorophyll can be stratified in the mixed layer defined by MLD_1. The 2008 spring bloom was dominated by the diatom *Asterionellopsis glacialis* (Twining *et al.*, 2014), and was likely terminated by iron limitation, even though diatoms consumed less than 1/3 of the mixed-layer dissolved iron inventory (Boyd *et al.*, 2012).

Conditions during 2012 (Figure 3, right-hand panels), were different, however. Upon arrival at the site, the water column was ~0.5 ºC cooler than in 2008, and there was little evidence of stratification (both MLD_1 and MLD_2 were at about 350 m). The wind was weaker than in 2008, with 4 relatively calm periods (19 September, 21-24 September, 28-29 September, and 3-5 October) during which the wind stress was less than 0.1 N m^{-2} (corresponding to a wind speed of ~8 m s^{-1}). These calm periods were interspersed with periods where the wind stress rose to 0.4 N m^{-2} (~16 m s^{-1}).

During the first calm period (19 September) there was a small (~0.1 ºC) increase in surface temperature, with an associated shoaling of MLD_2. This temperature signal was mixed down by stronger winds the next day. The second calm period from 21-24 September, lasted considerably longer, but surprisingly, SST did not show any substantial response, rising by only 0.03 ºC during this event (in comparison SST rose 0.35 ºC during a 2-day calm period in 2008). During this second calm period there was no apparent increase in stratification - both MLD_1 and MLD_2 remained at about 350 m. Paradoxically, SST started to rise as the wind increased on 25 September, and continued to increase even as the winds strengthened through 27 September. Also, counter intuitively, stratification increased during these stronger winds, with MLD_2

starting to shoal from about 26 September. The third calm period (28-29 September) was short lived, but substantial surface warming occurred during this calm when SST rose by ~0.5 ºC. This increase in SST was accompanied by a shoaling in MLD_2 (and temporarily MLD_1).

As in 2008, the onset of stratification appeared to trigger a phytoplankton response in the upper 100 m. From about 28 September, there was a general trend for chlorophyll to become more stratified in the water column, with surface chlorophyll concentration rising to ~0.8 mg m^{-3} by the end of the cruise.

Compared to 2008, there was about 10% less total chlorophyll in the water column, with mean ± standard deviation of $C_{0/300}$ = 28.6 ± 3.8 mg m^{-2} (cf. 31 ± 6.7 mg m^{-2} in 2008). As in 2008, $C_{0/300}$ changed little during the cruise and was uncorrelated with C_0 (r^2 = 0.16).

During both cruises, $C_{0/300}$ showed much less variation than C_0. This suggests that the photic zone was shallower than the depth to which phytoplankton were being mixed. Thus, as the vertical mixing ceased (i.e., as MLD_2 shoaled) phytoplankton below the mixed layer did not survive, and increased biomass at the surface was compensated for by losses at depth (it is probably coincidental that the losses almost exactly balanced the increased production). When MLD_2 deepened (e.g., from 26 Sept 2008), mixing distributed the phytoplankton throughout the deepening mixed layer so that the surface concentration decreased even though the total amount of phytoplankton in the water column stayed approximately the same (e.g., Evans & Parslow, 1985).

The 2008 and 2012 cruises were different in their nutrient evolution (Figure 4). In 2008, the macronutrients (nitrate, silicate and phosphate) were substantially depleted in the upper 100 m on arrival at the site. The wind event 19-20 September mixed up nutrients from below the nutricline, but these were then consumed by the production starting 23 September (Boyd *et al.*, 2012). Similarly it appears that the stronger winds towards the end of the cruise also mixed nutrients up into to the mixed layer.

In contrast, during 2012, nitrate plus nitrite and phosphate were relatively well mixed over the upper 300 m from the beginning of the cruise until they were

consumed by phytoplankton production above 100 m from about 28 September. Concentrations of nitrate plus nitrite (>4 µmolar) and phosphate (>0.4 µmolar) at the beginning of the cruise were typical of the deeper values seen in 2008.

Silicate, on the other hand, showed high levels (>2.3 µmolar) throughout the water column (except for the very upper few metres) on the first day of the cruise, but after that concentrations (~1.9 µmolar) dropped to less than half the deep values seen in 2008. Silicate was further depleted (to ~1.5 µmolar) during the increase in phytoplankton biomass starting ~28 September. Dissolved iron showed a pattern similar to that of silicate, with high values (~0.5 nmolar) throughout most of the water column on the first day, but then dropping to ~0.35 nmolar before being reduced to ~0.1 nmolar by the production starting ~28 September.

Even though depth-integrated chlorophyll stocks agreed to within 10% during both cruises (Figure 3D), the phytoplankton community structure and size-fractionated net primary production (NPP) were quite different (Figure 5).

During 2008, NPP was initially dominated by cells larger than 20 µm, and community NPP was 2875 to 4040 mg C m^{-2} d^{-1}. During the cruise both the portion of NPP due to cells larger than 20 µm and total community NPP decreased by a factor of more than 2, so that NPP was 1446 mg C m^{-2} d^{-1} at the end of the cruise.

In 2012, however, cells larger than 20 µm accounted for only 8-15% of NPP. NPP was 615 mg C m^{-2} d^{-1} initially and doubled to 1384 mg C m^{-2} d^{-1} at the end of the cruise (one third the maximum rate seen in 2008). The fate of the spring bloom in 2008 – as downward export or herbivory – is not known.

Early in 2012, picophytoplankton represented around 80% - 90% of NPP in the surface 50 m. This dominance was largely maintained until between 30 September and 5 October, when an increase in diatom abundance occurred (concurrent with the increase in C_0).

The >2 µm phytoplankton population consisted of a mix of small flagellates (2-20 µm), dinoflagellates and diatoms. The diatom populations included species of *Asterionellopsis*, *Cerataulina*, *Fragilaria*, *Corethron*, *Guinardia*, *Chaetoceros*, *Thalassiosira* and *Ditylum*. The silicoflagellate, *Dictyocha*, was also present. The dinoflagellates which initially outnumbered diatoms were dominated by *Ceratium* (*C. lineatum C. furca* and *C. fuscus*), and *Gymnodinium*, but also included some genera

which are known to be heterotrophic or mixotrophic (some with endosymbionts) including *Gyrodinium*, *Scrippsiella*, *Dinophysis*, *Protoperidinium* and *Prorocentrum.* On-board deck incubation experiments became diatom dominated primarily by the genus *Asterionellopsis*.

The dominance of large cells in the 2008 bloom and the high rates of NPP relative to the 2012 bloom indicate that the fate of this NPP was likely downward export, although we have no sediment trap data to test this.

Microzooplankton data from each cruise are shown in Figure 6. In 2008 microzooplankton levels were highest on arrival at station, concurrent with the high concentration of chlorophyll seen in the upper water column at that time (Figure 5). There was a general decrease in microzooplankton levels as this initial phytoplankton was mixed down, and then a delayed response of Aloricate ciliates (>20 µm) to the increase in primary biomass seen from 29 September. In 2012, there was a reasonably rapid increase in microzooplankton levels in response to the primary production starting ~28 September.

Heat and wind fluxes during 2012 cruise

A more detailed analysis of the upper water column during the 2012 cruise (Figure 7) explains why the water column did not stratify during the calm period 21-24 September, and why counter-intuitively, SST increased and the mixed layer shoaled when the winds increased from 25 September.

Prior to, and during, the 21-24 September calm, the winds were generally from the south, and the air was substantially colder than the ocean with an air-sea difference of -5 ºC on 21 September. About 24 September, the wind turned to become from the north, and as the wind speed increased, the air warmed to finally became warmer than the ocean about 27 September. Thus, the cool southerly airflow that dominated the region until ~27 September suppressed almost all ocean heating, with the net result that SST increased only marginally during the 21-24 September calm.

It was not until the air became warmer than the ocean on 27 September that SST increased, and the ocean began to stratify. SST peaked during the 28-29 September calm, and this period was characterised by increasing, but weak, stratification and shoaling MLD_2.

Mesoscale variability in 2012

Mesoscale spatial variability in both the physics and biology of the region will be aliased in the Lagrangian sampling, we can use the CTD data collected on the daily surveys to attempt to determine whether the conclusions based on the 3 am casts are likely to be impacted by this aliasing.

The horizontal scale of the eddy, and how close the 3 am casts were made to the eddy centre can be estimated from the daily shipboard ADCP surveys (Figure 8). The daily ADCP surveys did not always completely map the eddy (which was also evolving). However, inspection of the maps suggests that at least up until 26 September, the 3 am CTD cast was made within 2 to 3 km of the centre of the eddy. By 30 September, however, it appears that the Lagrangian Array was slipping towards the outside of the eddy.

Figure 9 shows the sea surface temperature, sea surface chlorophyll, and temperature and chlorophyll sections constructed from all casts. Temperature shows evidence of diurnal heating near the surface, with SST at noon on average 0.14 ºC warmer than at 3 am. The diurnal heating was uncorrelated with separation distance between 3 am and noon casts, and with time into the cruise. Early in the cruise this diurnal heating impacted MLD_2, but once the stratification strengthened there was no difference in MLD_2 between the night-time and day-time casts. Apart from the diurnal heating effects, the same progression from well-mixed to stratified conditions would have been observed had the 3 am casts been replaced with any cast taken on the same day, suggesting that spatial variability associated with the eddy was insufficient to alias the observed temporal evolution of the density structure significantly.

Surface chlorophyll shows quenching in the upper layers, with surface chlorophyll at noon being 0.19 mg m^{-3} lower on average than the previous 3 am cast. Although quenching was highest late in the cruise, it was also uncorrelated with the separation distance and time into the cruise. This quenching was severe enough that we cannot map chlorophyll across the eddy, but illustrates the importance of using the 3 am casts for this analysis.

405 ***Comparison of 2008 and 2012 years***

406 The shipboard observations show that in both 2008 and 2012, surface
407 phytoplankton concentration increased in response to the onset of weak stratification
408 (characterised by shoaling of MLD_2, but not MLD_1), although vertically-integrated
409 chlorophyll stocks remained relatively constant. The main differences are that in 2012
410 there the onset of stratification was delayed by the presence of cool southerly winds.

411 Figure 10 puts the cruise observations into context of the physical forcing
412 during their respective years, showing sea surface chlorophyll, C_0, from MODIS,
413 temperature from Argo, and NHF and wind stress from NCEP reanalyses. We also
414 show the rate of surface chlorophyll production, $r = \partial \ln(C_0)/\partial t$. The NHF and wind
415 stress have been smoothed in time to approximately match the smoothing inherent in
416 the compositing of the satellite data. We also show the climatological annual cycles
417 for NHF, wind stress, sea surface chlorophyll, and r (see Methods).

418 Although not shown here, of all years between 2002 and 2012, C_0 during 2008
419 was the closest to the climatological annual cycle. Thus 2008 can be regarded as a
420 canonical year, showing both autumn and spring blooms (Figure 10A), although the
421 spring bloom was initially much stronger than climatology.

422 In contrast, 2012 showed little evidence of an autumn bloom, and instead of
423 showing the canonical decrease during winter, C_0 slowly increased from late summer
424 until late spring, but with 1-2 month oscillations (events) superimposed on this rise.
425 The last of these was largest when C_0 peaked at about 60% above the climatological
426 value.

427 The Argo profiles (Figure 10C) were too infrequent to fully resolve the time
428 sequence of temperature, but surface waters were ~20 ºC in summer and ~13 ºC in
429 winter in both years. The mixed layer depth, MLD_1, was typically about 50 m during
430 summer and began to deepen in April, with deepest MLD_1 in late August. In both
431 years, the cruises took place a month to 6 weeks after the time of deepest observed
432 MLD_1.

433 The NHF in both years (Figure 10D) peaked in June and crossed zero in mid-
434 September, about a month to 6 weeks after the deepest MLD (i.e., the deepest mixed

435 layer occurs a month or so before the ocean stops cooling). In each year, the NHF
436 showed month to month variability about the climatological annual cycle, with the
437 longest departure from normal being in 2012 when NHF was consistently lower than
438 climatology during July and August.

439 The climatological cycle of wind stress has a minimum in summer and peaks in
440 June (Figure 10E). Both 2008 and 2012 showed large oscillations about this cycle,
441 this reflects that fact that while winds are generally stronger in winter than in summer,
442 the wind field in this region is highly variable.

443 Because the sea surface chlorophyll growth rate, r, is the time derivative of
444 $\ln C_0$, even the climatological value is quite noisy although it shows positive values
445 from February to April reflecting the autumn bloom, negative values from May to
446 July and then positive values from August to October. Compared this climatology, r
447 in both years shows large oscillations, but in 2008 showed peaks in autumn associated
448 with the autumn bloom and in September associated with the spring bloom (Figure
449 10F). In 2012, there was a series of oscillations in r from August to October
450 reflecting the series of blooms seen in sea surface chlorophyll.

451 ***2012 Anomalies***

452 A more detailed analysis of the variability in 2012 can be made by considering
453 the departures from the climatological mean.

454 Figure 11 shows the surface chlorophyll, C_0, the growth term, $r = \partial\, lnC_0 / \partial t$,
455 and the NHF anomaly, $\Delta_{NHF} = NHF - \overline{NHF}$, and wind stress anomaly, $\Delta_\tau = \tau - \tilde{\tau}$
456 (where the overbar indicates the climatological value).

457 Vertical lines on all plots indicate 9 local maxima in r, which correspond to
458 with the leading edges of individual events in C_0.

459 In 5 out of the 9 instances (March, May, June, early September and October as
460 indicated by dashed lines) the maxima in r occurred when the wind stress and NHF
461 anomalies were at or near local positive maxima. This suggests for these 5 instances,
462 the peaks in surface chlorophyll were driven by higher than normal vertical mixing
463 and more convective overturn than normal. We refer to these events as mixing events.

In 4 of the 9 instances (February, August, late September, and November as indicated by solid vertical lines), the maxima in r occurred when both the heat flux anomaly and the wind stress anomaly were negative. This suggests that the corresponding peaks in surface chlorophyll were driven by increased stability due to reduced turbulence and/or more heat into the ocean than normal. We refer to these events as stability events.

Thus Figure 11 suggests that unlike a canonical year, sea surface chlorophyll concentration in 2012 showed a series of winter and spring events modulated by the local wind and heat flux. The event in early October just reached our 0.5 mg m^{-3} spring bloom threshold, but the peak in surface chlorophyll was not until late October. We return to the implications of this findings later, but first investigate whether the results from the nominal site are representative of the region as a whole.

Spatial scales of surface chlorophyll from MODIS

To address the question of how representative the nominal site is of the region in general, Figure 12 shows 8-day composite images of C_0 from MODIS for various dates in 2008 and 2012, along with the climatological values for the same dates.

Perhaps the most striking feature of these images is the high degree of patchiness in C_0, with the obvious implication that had a different experimental site been chosen, a different sequence of events may have been computed for each year. Nevertheless, there are some broad conclusions that are supported by Figure 12.

The climatology shows surface chlorophyll concentrations are generally low throughout the region in mid-August. A spring bloom starts in late September and peaks about a month later. By late-November, surface chlorophyll levels decrease to low summer values everywhere except for over the Chatham Rise. The influence of the warm core Wairarapa Eddy (e.g., Roemmich & Sutton, 1998) appears to be strong with reduced surface biomass within the eddy, presumably because of deeper pycnocline (i.e., deeper nutricline) in summer and hence less nutrient availability (e.g., Bradford *et al.*, 1982). Surface chlorophyll concentration is highest along the Subtropical Front along the Chatham Rise in summer. The climatology is consistent

493 with previous work on primary production in the region (e.g., Bradford *et al.*, 1982,
494 Chiswell *et al.*, 2013).

495 Compared to climatology, surface chlorophyll in 2008 shows near-identical
496 sequence, except that values are much higher than expected early in the spring bloom
497 (also seen in Figure 10). The influence of the Wairarapa Eddy is clear, and the spatial
498 structure of surface chlorophyll matches climatology well.

499 In contrast, the 2012 images paint an entirely different picture of surface
500 chlorophyll showing a series of 'blooms and busts', some of which are quite limited in
501 areal extent. Surface chlorophyll at the site showed a small event in mid-August (the
502 5^{th} of the 9 anomalies discussed earlier). The composite image for 17 August 2012
503 shows that this bloom was likely limited spatially to a region west of East Cape, and
504 that much of the rest of the region showed chlorophyll levels typical of mid-winter
505 (although the considerable cloud cover means we cannot be sure of this). A little over
506 a month later, the 26 September 2012 image coincides with the mid-point of the
507 cruise, and surface chlorophyll shows levels throughout the region that are
508 substantially lower than climatology. By 4 October a bloom had developed over most
509 of the region (except at the experimental site) that brought surface chlorophyll to near
510 climatology. However, by 20 October (which should be near the peak spring bloom in
511 the climatology) this bloom had disappeared and surface chlorophyll was well below
512 climatology over most of the region. At the experimental site, surface chlorophyll rose
513 rapidly about this time (Figure 10A) and the following 8-day satellite composite (28
514 October) shows an extensive region where surface chlorophyll exceeds 1 mg m^{-3}. On
515 21 November, surface chlorophyll over most of the region was near climatology, but
516 the time series at the site show a small positive anomaly developing (Figure 11),
517 which appears to be a relatively small localised feature.

DISCUSSION

518 The main findings of this work are that in 2008, the timing of the surface
519 chlorophyll concentration at the experimental site followed the climatological annual
520 cycle for this location, although the spring bloom was stronger than climatology. In
521 contrast, in 2012, surface chlorophyll concentration showed little evidence of an
522 autumn bloom and showed a series of winter and spring events modulated by the local
523 wind and heat flux that did not become fully developed blooms until October. The
524 satellite imagery suggests these findings apply to a broad region east of the North

525 Island, although there was substantial spatial patchiness in the surface chlorophyll
526 levels.

527 The 2012 sequence of events in surface chlorophyll illustrates that surface
528 chlorophyll growth can be categorised by what we term either mixing or stability
529 events. Mixing events mix up any deep chlorophyll maximum and/or inject new
530 nutrients into the surface layers allowing increased production (e.g., Findlay *et al.*,
531 2006). Stability events allow phytoplankton to remain in the photic zone and grow
532 (e.g., Chiswell *et al.*, 2015b, Huisman *et al.*, 1999, Taylor & Ferrari, 2011).

533 Autumn blooms are typically mixing events, and the 2008 autumn bloom was a
534 mixing event induced by increased wind stress and the onset of convective overturn at
535 the end of summer.

536 Spring blooms are typically stability events, and there is little doubt that the
537 2008 spring bloom was a mixing event. Surface chlorophyll started to increase at
538 about the time of deepest MLD – almost a month before the NHF changed sign, and
539 the peak of the bloom occurred after the onset of stratification. This timing is
540 consistent with the timeline for spring blooms suggested by Chiswell *et al.* (2015b)
541 who note that in a 1-d system, the mixed layer must start to shoal before the NHF
542 changes sign.

543 The 2008 spring bloom had been underway for some time before the 2008
544 cruise, hence the partial drawdown of nitrate and dissolved iron, and high zooplankton
545 levels seen at the start of the cruise. This conclusion is also supported by Ellwood *et*
546 *al.* (2015) who found dissolved iron within the surface mixed layer was isotopically
547 heavy. (Isotopically heavy iron occurs when the lighter iron isotopes are selectively
548 removed from the water column due to the uptake by phytoplankton.) Strong winds
549 about 19 September mixed down this early bloom, and resupplied the mixed layer
550 with nutrients to allow the second bloom seen near 25 September. It appears that even
551 in canonical years there are episodic interruptions to the bloom dynamics.

552 The first indication that 2012 was anomalous was the lack of an autumn bloom.
553 At the beginning of March, there was a period of stronger than normal winds and
554 more cooling than normal (event 2), which would normally be expected to drive an
555 autumn bloom. However, these conditions were replaced by a period of negative NHF
556 anomaly which lasted throughout April. This suggests that during late March and

April there was less cooling than normal, and that this was sufficient to prevent an autumn bloom from occurring.

The progression of events over the rest of 2012 was also different from canonical. The series of mixing events seen in May, June and early September 2012, suggest that even in winter, increased surface chlorophyll can be initiated by increased mixing. Since deep chlorophyll maxima are generally not seen in winter (Chiswell, 2011) these winter mixing events were likely driven by entrainment of nutrients leading to increased production in the mixed layer.

Three winter/spring stability events occurred in August, late September and November 2012 (events 5, 7 and 9). The late September event was observed during the cruise when surface chlorophyll rose in response to increased stratification (Figure 3). It is likely the November bloom was triggered in a similar fashion, but the August event took place while the NHF was still positive (although anomalously weak). It seems unlikely that water column stratification could occur when there was still cooling, and so without *in situ* data for this event, we can only speculate that this was an event triggered by reduced turbulence (e.g., Huisman *et al.*, 1999).

Perhaps the most interesting observation of 2012 is that the largest peak in surface chlorophyll, in late October 2012, was likely driven by increased mixing and paradoxically was therefore propelled by mechanisms more appropriate for an autumn bloom rather than a spring bloom.

Thus, it seems that in 2012, the spring bloom started with an increase in stratification leading to a conventional bloom in early October, but increasing winds and decreased surface heating led to this bloom initially being mixed out, and then replaced with a mixing bloom in late October.

It is not clear from our observations why 2012 should have been such an anomalous year. SST at the site was cooler than climatology throughout most of 2012 (Figure 10), and 2012 was the third coolest year between 1985 and 2017 (Figure 13). This is despite the fact that, according to NOAA (www.ncdc.noaa.gov/sotc/global/201213), the global average SST for 2012 was 0.45°C above the 20’th century mean (and at that time, 2012 was the 10’th warmest year on record). At the experimental site there is no clear relationship between El Nino and SST anomaly – for example, SST anomaly was negative during the during

589 the 1992/93 El Nino, but positive during the 1997/1998 El Nino years. There was
590 nothing particularly anomalous about either the annual wind stress or net heat flux
591 during 2012, and there was no clear relationship between either of these quantities and
592 SST (Figure 13). These observations suggest that in 2012, while SST east of New
593 Zealand did not follow the global trends, it was also not driven solely by local forcing
594 and thus was a response to a complex set of forcing that is beyond the scope of this
595 article to determine.

596 It likely that the cooler than normal conditions during 2012 played a role in
597 the mixing spring bloom in that year, because these imply a weaker than normal
598 thermocline. However, how common mixing spring blooms are, and whether they
599 have a significant impact on the annual net primary production is uncertain, and these
600 questions remain topics for future research.

CONCLUSION

601 The temporal evolution of stability during bloom development is critical.
602 Surface chlorophyll blooms can be triggered by loss of stability when increased wind
603 stress and convective overturn lead to mixing up of the deep chlorophyll maximum
604 and or increase nutrients into the mixed layer, or they can also be triggered by
605 increased stability when decreased wind stress and decreased convective overturn lead
606 to conditions when phytoplankton remain in the photic zone. Traditionally, autumn
607 blooms are considered to be triggered by decreasing stability, and spring blooms are
608 considered to be triggered by increasing stability. This research suggests that this
609 paradigm does not always hold, and that there is at least one case where the spring
610 bloom is triggered by loss of stability. We can for now only speculate how common
611 such blooms are, whether this mechanism drives more productive spring blooms than
612 those driven by increased stability.

ACKNOWLEDGEMENTS

613 We thank all those involved during the two cruises, including the Master and crew of
614 RV ‘Tangaroa’ for their contribution to the data collection. We thank Karen Robinson
615 and Scott Nodder for shore-based analyses and constructive comments on this work.
616 Simon Wood provided daily satellite images to aid us in locating the eddy.

The Argo and MODIS programs are thanked for their efforts in maintaining these programs and making the data freely available We thank three reviewers for their careful and conscientious reviews.

FUNDING

The two cruises and support for S.M.C., K.S. and P.W.B. were funded by the New Zealand Government through a grant to the National Institute of Water and Atmospheric Research. R.S. and M.J.E. were also supported by the Australian Research Council [grants DP110100108, DP0770820, and DP130100679]; A.M. was supported by the Natural Environmental Research Council [grants NERC NE/H004475/1 awarded to Maeve Lohan]. S.G.S. was supported by funding to Environment Laboratories by the Government of the Principality of Monaco.

All data used in this project are freely available. Some data (largely the CTD data) are available via the New Zealand Ocean Data Network (https://nzodn.nz), but all data will be provided on request.

REFERENCES

Boyd, P. W., Strzepek, R., Chiswell, S., Chang, H., Debruyn, J. M., Ellwood, M., Keenan, S., King, A. L., Maas, E. W., Nodder, S., Sander, S. G., Sutton, P., Twining, B. S., Wilhelm, S. W. and Hutchins, D. A. (2012) Microbial control of diatom bloom dynamics in the open ocean. *Geophysical Research Letters*, **39**.

Bradford, J. M., Heath, R. A., Chang, F. H. and Hay, C. H. (1982) The effect of warm-core eddies on oceanic productivity off northeastern New Zealand. *Deep Sea Research Part A. Oceanographic Research Papers*, **29,** 1501-1516.

Brody, S. R., Lozier, M. S. and Dunne, J. P. (2013) A comparison of methods to determine phytoplankton bloom initiation. *Journal of Geophysical Research: Oceans*, **118,** 2345-2357.

Chandrasekhar, A., Thalayappil, S. R. S., Boyd, P. W., Ellwood, M. J., Milne, A., Chiswell, S. M. and Sander, S. G. (2018) The distribution of Fe-binding ligands during the FeCycle III study of subtropical iron biogeochemical cycling, evidence for hydrothermal iron input. *TBD*.

Chiswell, S. M. (2011) Annual cycles and spring blooms in phytoplankton: don't abandon Sverdrup completely. *Marine Ecology Progress Series*, **443,** 39-50.

Chiswell, S. M., Bostock, H. C., Sutton, P. J. H. and Williams, M. J. M. (2015a) Physical oceanography of the deep seas around New Zealand: a review. *New Zealand Journal of Marine and Freshwater Research*, **49,** 286-317.

Chiswell, S. M., Bradford-Grieve, J., Hadfield, M. G. and Kennan, S. C. (2013) Climatology of surface chlorophylla, autumn-winter and spring blooms in the southwest Pacific Ocean. *Journal of Geophysical Research: Oceans*, **118,** 1003-1018.

Chiswell, S. M., Calil, P. H. R. and Boyd, P. W. (2015b) Spring blooms and annual cycles of phytoplankton: a unified perspective. *Journal of Plankton Research*, **37,** 500-508.

Cole, H. S., Henson, S., Martin, A. P. and Yool, A. (2015) Basin-wide mechanisms for spring bloom initiation: how typical is the North Atlantic? *ICES Journal of Marine Science: Journal du Conseil*, **72,** 2029-2040.

Dutkiewicz, S., Follows, M., Marshall, J. and Gregg, W. W. (2001) Interannual variability of phytoplankton abundances in the North Atlantic. *Deep-Sea Research Part Ii-Topical Studies in Oceanography*, **48,** 2323-2344.

Ellwood, M. J., Hutchins, D. A., Lohan, M. C., Milne, A., Nasemann, P., Nodder, S. D., Sander, S. G., Strzepek, R., Wilhelm, S. W. and Boyd, P. W. (2015) Iron stable isotopes track pelagic iron cycling during a subtropical phytoplankton bloom. *Proceedings of the National Academy of Sciences of the United States of America*, **112,** E15-E20.

Esaias, W. E., Abbott, M. R., Barton, I., Brown, O. B., Campbell, J. W., Carder, K. L., Clark, D. K., Evans, R. H., Hoge, F. E., Gordon, H. R., Balch, W. M., Letelier, R. and Minnett, P. J. (1998) An overview of MODIS capabilities for ocean science observations. *Geoscience and Remote Sensing, IEEE Transactions on*, **36,** 1250-1265.

Evans, G. T. and Parslow, J. S. (1985) A Model of Annual Plankton Cycles. *Biological Oceanography*, **3,** 327-347.

Fairall, C. W., Yang, M., Bariteau, L., Edson, J. B., Helmig, D., Mcgillis, W., Pezoa, S., Hare, J. E., Huebert, B. and Blomquist, B. (2011) Implementation of the

Coupled Ocean-Atmosphere Response Experiment flux algorithm with CO2, dimethyl sulfide, and O3. *Journal of Geophysical Research: Oceans,* **116,** .

Findlay, H. S., Yool, A., Nodale, M. and Pitchford, J. W. (2006) Modelling of autumn plankton bloom dynamics. *Journal of Plankton Research,* **28,** 209-220.

Floor, G. H., Clough, R., Lohan, M. C., Ussher, S. J., Worsfold, P. J. and Quetel, C. R. (2015) Combined uncertainty estimation for the determination of the dissolved iron amount content in seawater using flow injection with chemiluminescence detection. *Limnol Oceanogr Methods,* **13,** 673-686.

Gould, W. J. and Turton, J. (2006) Argo – Sounding the oceans. *Weather,* **61,** 17-21.

Hall, J. A. and Safi, K. (2001) The impact of in situ Fe fertilisation on the microbial food web in the Southern Ocean. *Deep Sea Research Part II: Topical Studies in Oceanography,* **48,** 2591-2613.

Henson, S., Robinson, I., Allen, J. and Waniek, J. (2006) Effect of meteorological conditions on interannual variability in timing and magnitude of the spring bloom in the Irminger Basin, North Atlantic. *Deep Sea Research Part I: Oceanographic Research Papers,* **53,** 1601-1615.

Henson, S. A., Dunne, J. P. and Sarmiento, J. L. (2009) Decadal variability in North Atlantic phytoplankton blooms. *Journal of Geophysical Research: Oceans,* **114,** C04013.

Huisman, J., Van Oostveen, P. and Weissing, F. J. (1999) Critical depth and critical turbulence: Two different mechanisms for the development of phytoplankton blooms. *Limnology and Oceanography,* **44,** 1781-1878.

Kara, A. B., Wallcraft, A., Metzger, E. J., Hurlburt, H. and Fairall, C. W. (2007) Wind Stress Drag Coefficient over the Global Ocean. *Journal of Climate,* **20,** 5856-5864.

Laws, E. A. (1991) Photosynthetic quotients, new production and net community production in the open ocean. *Deep Sea Research Part A. Oceanographic Research Papers,* **38,** 143-167.

Lebaron, P., Parthuisot, N. and Catala, P. (1998) Comparison of Blue Nucleic Acid Dyes for Flow Cytometric Enumeration of Bacteria in Aquatic Systems. *Applied Environmental Microbiology* **64,** 1725-1730.

Levy, M. (2015) Exploration of the critical depth hypothesis with a simple NPZ model. *ICES Journal of Marine Science*.

Müller, P., Li, X.-P. and Niyogi, K. K. (2001) Non-Photochemical Quenching. A Response to Excess Light Energy. *Plant Physiology,* **125,** 1558-1566.

Obata, H., Karatani, H. and Nakayama, E. (2002) Automated determination of iron in seawater by chelating resin concentration and chemiluminescence detection. *Analytical Chemistry,* **65,** 1524-1528.

Parsons, T. R., Maita, Y. and Lalli, C. M. (1984) 4.1 - Determination of Chlorophylls and Total Carotenoids: Spectrophotometric Method. In: T. R. Parsons, Y. Maita and C. M. Lalli (eds) *A Manual of Chemical & Biological Methods for Seawater Analysis.* Pergamon, Amsterdam, pp. 101-104.

Pickmere, S. E. (1998) Biological effects of cross-shelf water transfer programme nutrient report. NIWA Internal Report, pp. 5.

Putt, M. and Stoecker, D. K. (1989) An experimentally determined carbon : volume ratio for marine “oligotrichous” ciliates from estuarine and coastal waters. *Limnology and Oceanography,* **34,** 1097-1103.

Reynolds, R. W., Smith, T. M., Liu, C., Chelton, D. B., Casey, K. S. and Schlax, M. G. (2007) Daily High-Resolution-Blended Analyses for Sea Surface Temperature. *Journal of Climate,* **20,** 5473-5496.

728 Roemmich, D. and Sutton, P. J. H. (1998) The mean and variability of ocean
729 circulation past northern New Zealand: determining the representativeness of
730 hydrographic climatologies. *Journal of Geophysical Research,* **103,** 13041-
731 13054.
732 Smayda, T. J. (1997) What is a bloom? A commentary. *Limnology and*
733 *Oceanography,* **42,** 1132-1136.
734 Sverdrup, H. (1953) On Conditions for the Vernal Blooming of Phytoplankton.
735 *Journal du Conseil - Conseil International pour l'Exploration de la Mer* **18,**
736 287-295.
737 Taylor, J. R. and Ferrari, R. (2011) Shutdown of turbulent convection as a new
738 criterion for the onset of spring phytoplankton blooms. *Limnology and*
739 *Oceanography,* **56,** 2293-2307.
740 Twining, B. S., Nodder, S. D., King, A. L., Hutchins, D. A., Lecleir, G. R., Debruyn,
741 J. M., Maas, E. W., Vogt, S., Wilhelm, S. W. and Boyd, P. W. (2014)
742 Differential remineralization of major and trace elements in sinking diatoms.
743 *Limnology and Oceanography,* **59,** 689-704.
744 Westberry, T. K., Schultz, P., Behrenfeld, M. J., Dunne, J. P., Hiscock, M. R.,
745 Maritorena, S., Sarmiento, J. L. and Siegel, D. A. (2016) Annual cycles of
746 phytoplankton biomass in the subarctic Atlantic and Pacific Ocean. *Global*
747 *Biogeochemical Cycles,* **30,** 175-190.
748

FIGURES

Figure 1. Study region east of the North Island of New Zealand. Locations of 3 am casts made during spring bloom cruises in 2008 (red squares) and 2012 (blue squares) are superimposed on mean sea surface chlorophyll, C_0, derived from MODIS aqua ocean colour satellites. The 1000 m isobath is shown as a dashed line and the centre of the Wairarapa Eddy is labelled WE. Also shown are the locations of 42 Argo profiles in 2008 (solid red circles) and 23 profiles in 2012 (blue circles) made within 125 km of the nominal experimental site.

Figure 2. Locations of CTD casts made during the 2008 and 2012 spring bloom cruises. Blue squares show casts made at 3 am, red squares show casts made at noon (no noon casts were made in 2008) and green circles show other casts. The path of the Lagrangian array in 2012 is shown as a blue line.

Figure 3. Shipboard data from 2008 and 2012 cruises. (**A**) Wind stress, τ, numbers 1 to 4 in 2012 refer to the calm periods discussed in the text; (**B**) Sea surface temperature, T_0; (**C**) Temperature, T, from 3 am CTD casts (note different scales for each year); (**D**) Surface and depth-integrated chlorophyll from the 3 am CTD casts. Surface chlorophyll, C_0, is taken as the average over the top 5 m, and the depth-integrated chlorophyll, $C_{0/300}$, is integrated over the top 300 m; (**E**) Chlorophyll, C, section from the 3 am CTD casts. Two estimates of the mixed layer depth, MLD_1 and MLD_2, based on density differences of 0.125 and 0.025 kg m^{-3}, respectively (see Methods), are superimposed on the temperature and chlorophyll. Panels relating to 2008 data have been adapted from Chiswell (2011).

Figure 4. Nutrients during the 2008 and 2012 cruises from upcast water samples taken on the 3 am CTD casts. Two estimates of the mixed layer depth, MLD_1 and MLD_2, based on density differences of 0.125 and 0.025 kg m^{-3}, respectively (see Methods), are superimposed on the chlorophyll sections. (**A**) Wind stress, τ (as in Figure 3); (**B**) Chlorophyll, C; (**C**) Nitrate, NO_3, for 2008, and Nitrate plus Nitrite, $NO_3 + NO_2$, for 2012; (**D**) Silicate, SiO_3; (**E**) Phosphate, PO_4; and (**F**) Dissolved iron, dFe, taken from trace-metal samples.

Figure 5. Metrics of phytoplankton biomass and productivity for the 2008 and 2012 cruises. (**A**) Percentage of Net Primary Production (NPP) by cells larger than 20 µm; (**B**) Community NPP (cells larger than 0.2 µm); and (**C**) Chlorophyll, C (also shown in Figure 3, but with expanded depth scale). Dashed lines are mixed layer depth, MLD_2, based on density difference0.025 kg m^{-3}.

Figure 6. Microzooplankton from 2008 and 2012 cruises. (**A**) Wind stress, τ (as in Figure 3); (**B**) Aloricate ciliates <20 µm; (**C**) Aloricate ciliates >20 µm; (**D**) Tintinnids; (**E**) Mean Microzooplankton and chlorophyll concentrations over the top 100 m. For comparison, contours of chlorophyll (as seen in Figure 3) are shown in panels B to D.

Figure 7. Shipboard measurements from the 2012 cruise. (**A**) Wind speed, W ; (**B**) Wind direction, θ (180º indicates winds from the south); (**C**) Air minus sea temperature, $T_{air} - T_{sea}$; (**D**) Sea temperature, T_{sea} , from ships underway system, and sea surface temperature, T_0 , and chlorophyll, C_0 , from 3 am CTD casts.

Figure 8. Locations of CTD casts every second day during the 2012 spring bloom cruise, Blue squares show the 3 am casts, green squares show casts made between 12 hours before and 12 hours after the 3 am cast, along with the drifter track (green shows the full track, blue shows the track within 12 hours of the 3 am CTD cast), and surface velocities within 12 hours of the 3 am CTD cast from the shipboard Acoustic Doppler Current Profiler (ADCP, cyan vectors). Each panel is centred on the 3 am cast location and the dashed line shows a 10-km radius circle centred on that location.

Figure 9. (**A**) Sea surface temperature, T_0 , from CTD casts made in the 2012 cruise. The blue line connects T_0 from the 3 am casts, the green line connects T_0 from all CTD casts, and red squares show T_0 from the noon CTD casts (see Figure 2 for CTD locations); (**B**) Temperature section from all CTD casts made during the cruise. The dashed and solid lines are mixed layer depths MLD_1 and MLD_2 calculated using the 3 am casts as shown in Figure 3; (**C**) Sea surface Chlorophyll, C_0 , from CTD casts made in the 2012 cruise. The blue line connects C_0 from the 3 am casts, the green line connects C_0 from all CTD casts

and red squares shows C_0 from the noon CTD casts; (**D**) Chlorophyll, C, section from all CTD casts made during the cruise. The dashed and solid lines are the 0.5 and 0.25 mg m^{-3} contours shown in Figure 3.

Figure 10. Satellite and reanalysis data for 2008 and 2012. (**A**) Sea surface chlorophyll derived from MODIS satellite (blue line). Vertical dashed line indicates date of deepest mixed layer from Argo data. Horizontal dashed lines show 0.5 and 0.25 mg m^{-3} threshold criteria for spring and atumn blooms, respectively; (**B**) Sea surface temperature (SST) derived from AVHRR satellite (blue line); (**C**) Temperature derived from Argo profiles made within 125 km of the nominal site. Red and black dot-dashed lines indicate two estimates of the mixed layer depth, MLD_1 and MLD_2, based on density differences 0.125 and 0.025 kg m^{-3} (see Methods); (**C**) Net heat flux, NHF, from NCEP reanalysis (green); (**D**) Wind stress, τ, from NCEP reanalysis (blue); (**E**) Rate of change of surface chlorophyll, $r = \partial \ln C_0 / \partial t$. Vertical solid lines in all panels indicate beginning and ending of spring bloom cruises in 2008 and 2012. Grey lines in panels A, B, D and E show the climatological annual cycles of the respective quantities.

Figure 11. Satellite and reanalysis data for 2012. (**A**) Sea surface chlorophyll, C_0, derived from MODIS satellite data for the experimental site shown in Figure 1; (**B**) Rate of change of surface chlorophyll $r = \partial \ln C_0 / \partial t$; (**C**) Net Heat Flux anomaly, Δ_{NHF}, calculated as the difference between NHF during 2012 and the climatological value of NHF; (**D**) Wind stress annual anomaly, Δ_τ, calculated as the difference between τ during 2012 and the climatological value of τ. Vertical lines indicate periods of sustained surface chlorophyll increase as determined by local maxima in r. Solid lines indicate events driven by more heat entering the ocean than normal and less winds than normal and are referred to as ‘stability’ events. Dashed lines indicate evens driven by less heat entering the ocean than normal and/or higher wind stress than normal, and are referred to as ‘mixing’ events.

Figure 12. Sea surface chlorophyll derived from MODIS aqua satellite for selected days. Left-hand panels show the climatological values for the day of year. Centre and right-hand panels show 8-day composite sea surface chlorophyll for dates in 2008 and 2012. Discontinuities along 180º reflect the date-line change, and its impact on compositing data.

Figure 13. Annual anomalies for various quantities at the experimental site. For each year, the anomaly is calculated as the mean value of the quantity minus its climatology. (**A**) Sea surface temperature anomaly derived from AVHRR estimates of SST; (**B**) Wind stress anomaly derived from NCEP reanalysis; (**C**) Net heat flux (NHF) anomaly derived from NCEP reanalysis.

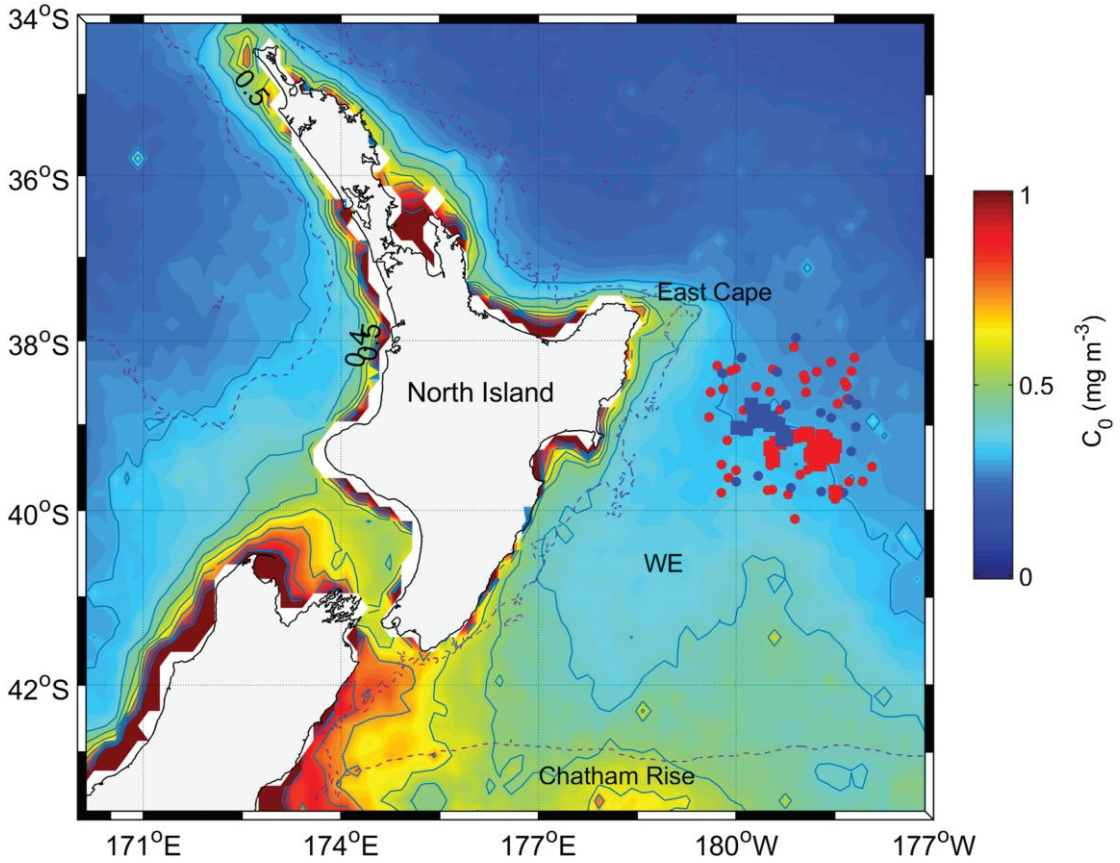
34°S
36°S
38°S
40°S
42°S
171°E
174°E
177°E
180°W
177°W
0.5
0.5
East Cape
North Island
WE
Chatham Rise
1
0.5
0
C0 (mg m-3)

849

850

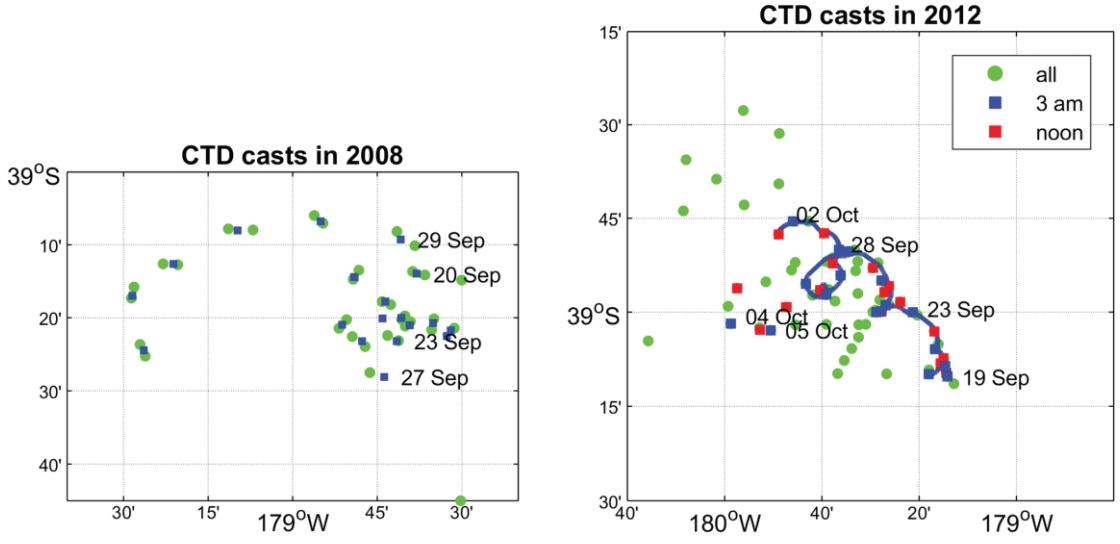
CTD casts in 2008
39°S
10'
20'
30'
40'
30'
15'
179°W
45'
30'
29 Sep
20 Sep
23 Sep
27 Sep
CTD casts in 2012
15'
30'
45'
39°S
15'
30'
40'
180°W
40'
20'
179°W
all
3 am
noon
02 Oct
28 Sep
04 Oct
05 Oct
23 Sep
19 Sep

851

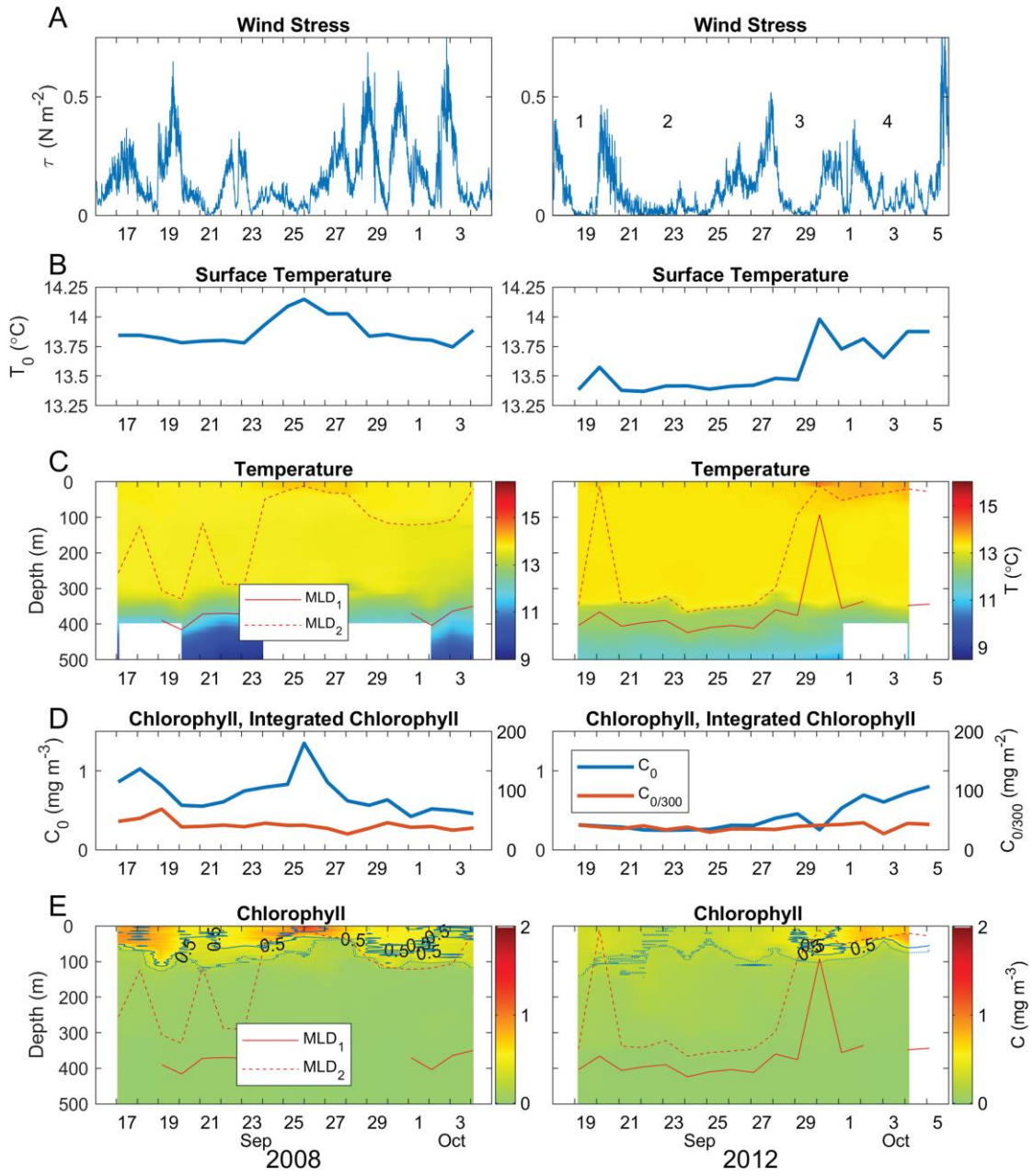
A
Wind Stress
Wind Stress
τ (N m-2)
B
Surface Temperature
Surface Temperature
T0 (°C)
C
Temperature
Temperature
Depth (m)
MLD1
MLD2
T (°C)
D
Chlorophyll, Integrated Chlorophyll
Chlorophyll, Integrated Chlorophyll
C0 (mg m-3)
C0
C0/300
C0/300 (mg m-2)
E
Chlorophyll
Chlorophyll
Depth (m)
MLD1
MLD2
C (mg m-3)
Sep
Oct
2008
2012

852
853

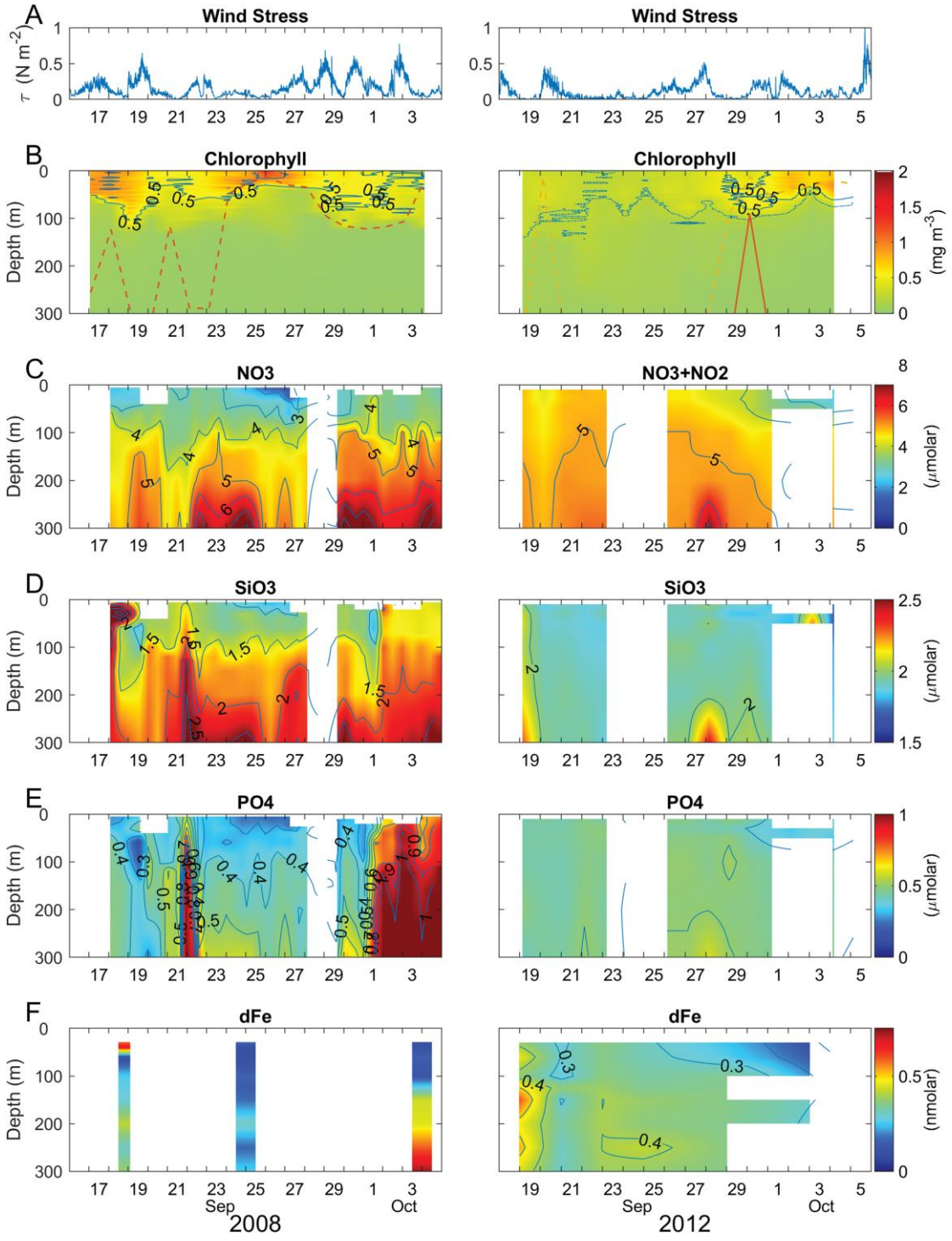
A
Wind Stress
τ (N m-2)
Wind Stress
B
Chlorophyll
Depth (m)
Chlorophyll
(mg m-3)
C
NO3
NO3+NO2
(μmolar)
D
SiO3
SiO3
(μmolar)
E
PO4
PO4
(μmolar)
F
dFe
dFe
(nmolar)
Sep
Oct
2008
2012

854

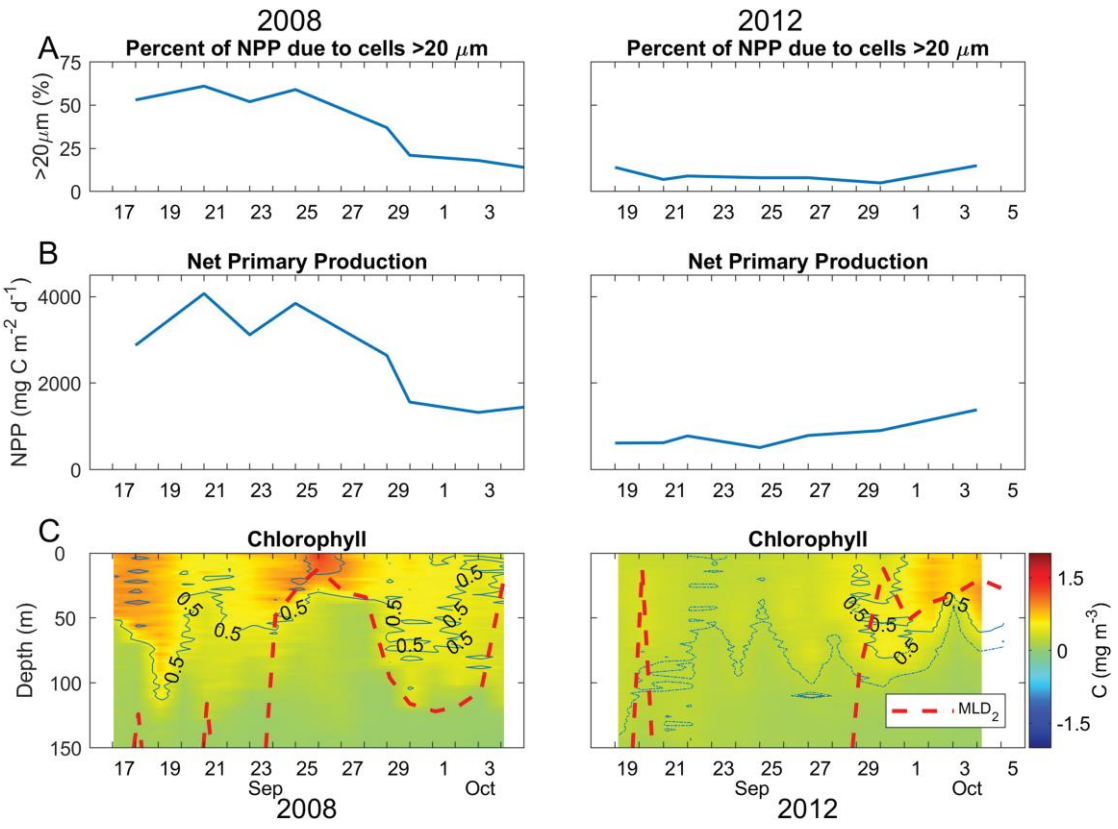
2008
2012
A
Percent of NPP due to cells >20 μm
>20μm (%)
B
Net Primary Production
NPP (mg C m-2 d-1)
C
Chlorophyll
Depth (m)
MLD2
C (mg m-3)
Sep
Oct

855

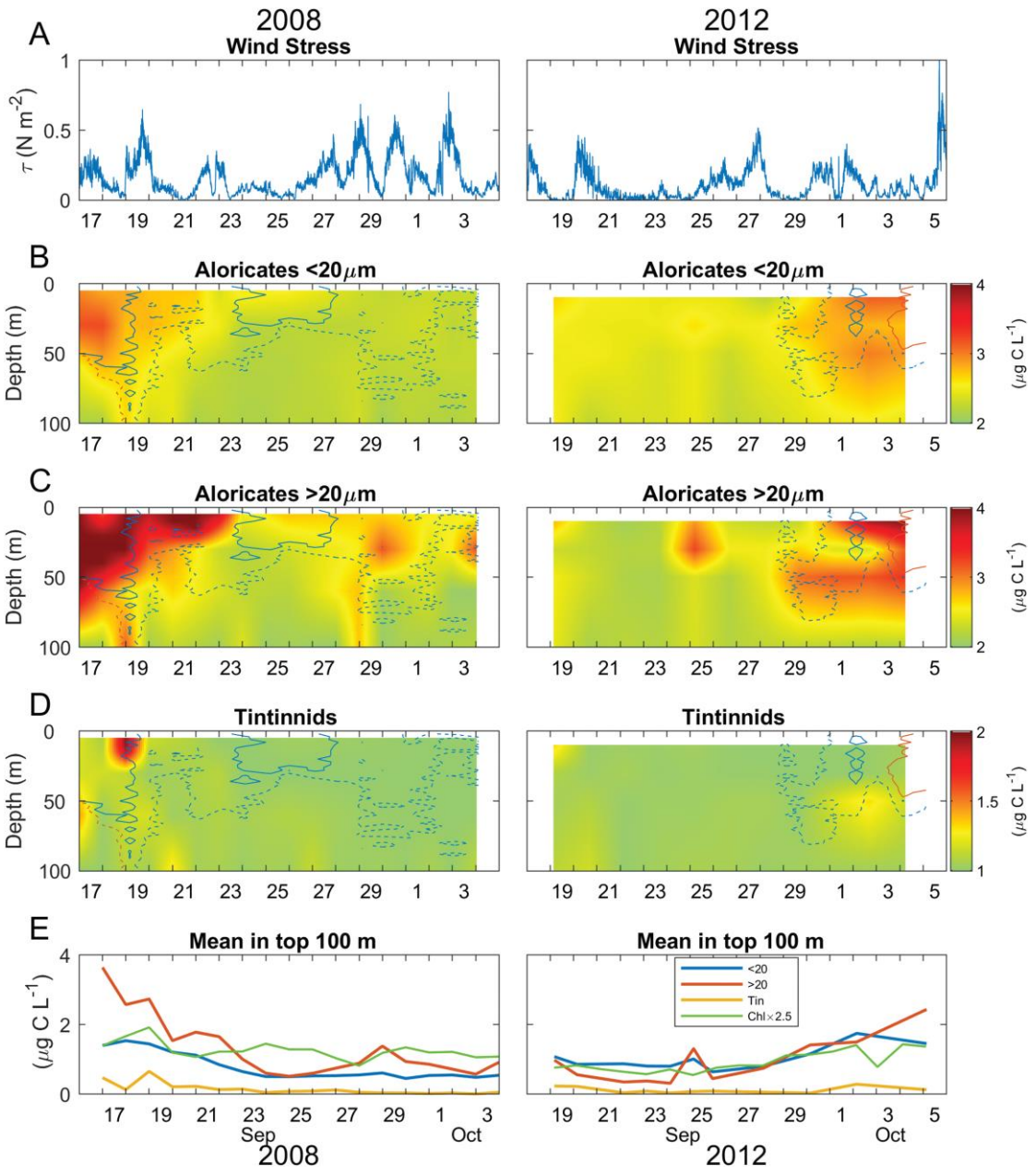
A
2008
Wind Stress
2012
Wind Stress
τ (N m-2)
B
Aloricates <20μm
Depth (m)
(μg C L-1)
C
Aloricates >20μm
D
Tintinnids
E
Mean in top 100 m
<20
>20
Tin
Chl×2.5
Sep
Oct
2008
2012

856

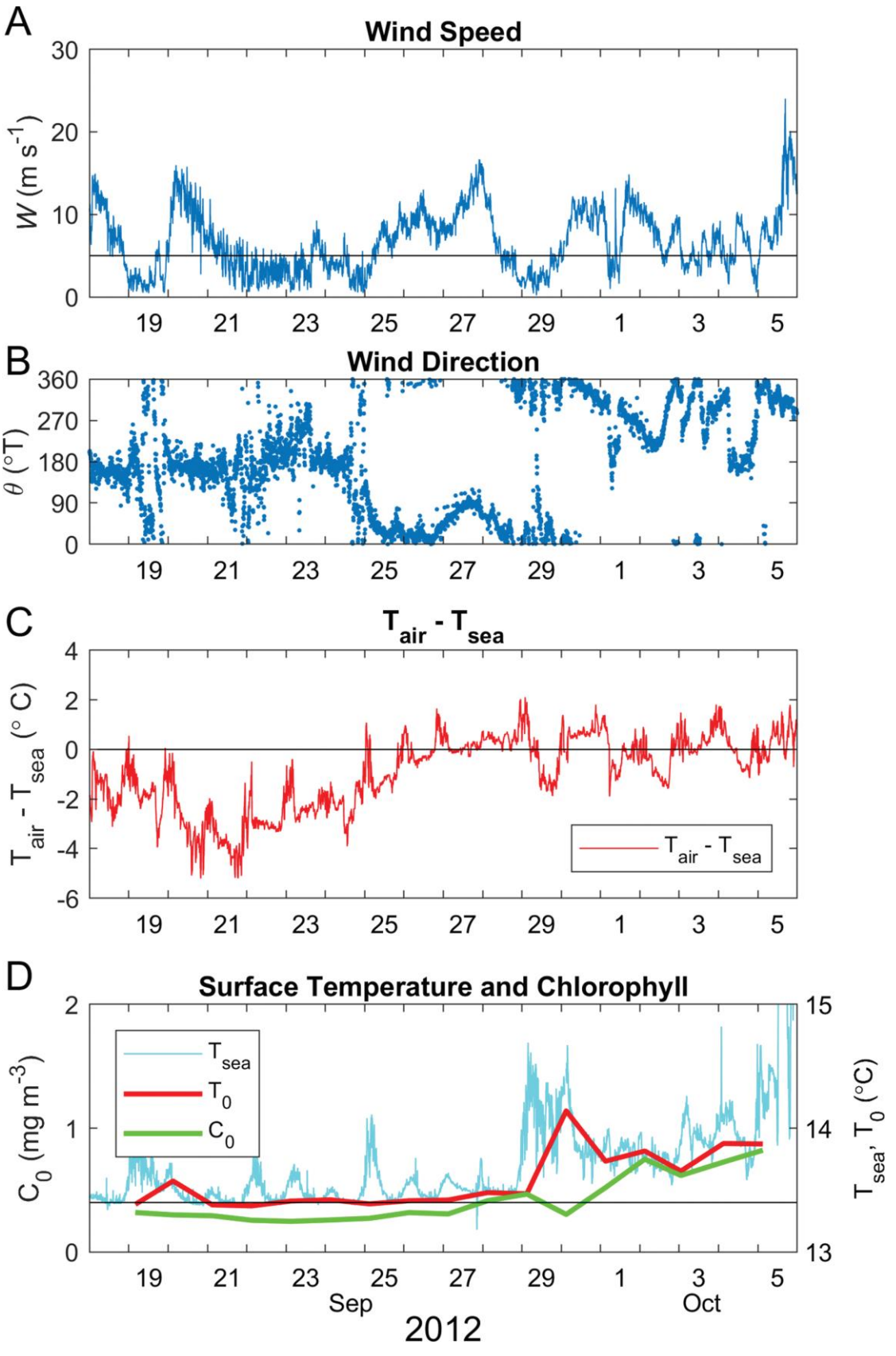
A
Wind Speed
W (m s-1)
30
20
10
0
19
21
23
25
27
29
1
3
5
B
Wind Direction
θ (°T)
360
270
180
90
0
C
Tair - Tsea
Tair - Tsea (° C)
4
2
0
-2
-4
-6
Tair - Tsea
D
Surface Temperature and Chlorophyll
C0 (mg m-3)
Tsea, T0 (°C)
Tsea
T0
C0
15
14
13
Sep
Oct
2012

857
858

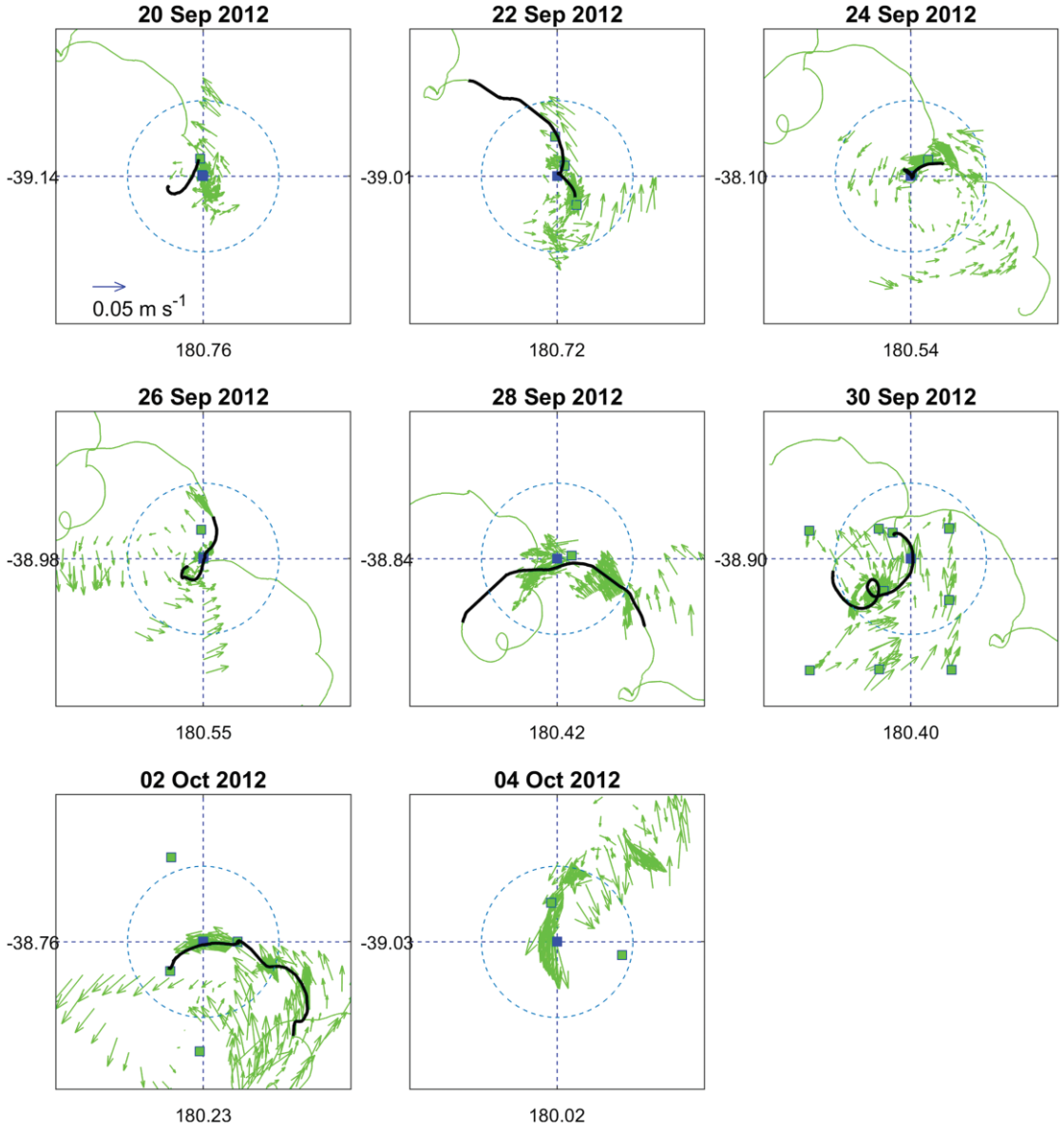
20 Sep 2012
22 Sep 2012
24 Sep 2012
-39.14
-39.01
-38.10
0.05 m s-1
180.76
180.72
180.54
26 Sep 2012
28 Sep 2012
30 Sep 2012
-38.98
-38.84
-38.90
180.55
180.42
180.40
02 Oct 2012
04 Oct 2012
-38.76
-39.03
180.23
180.02

859
860

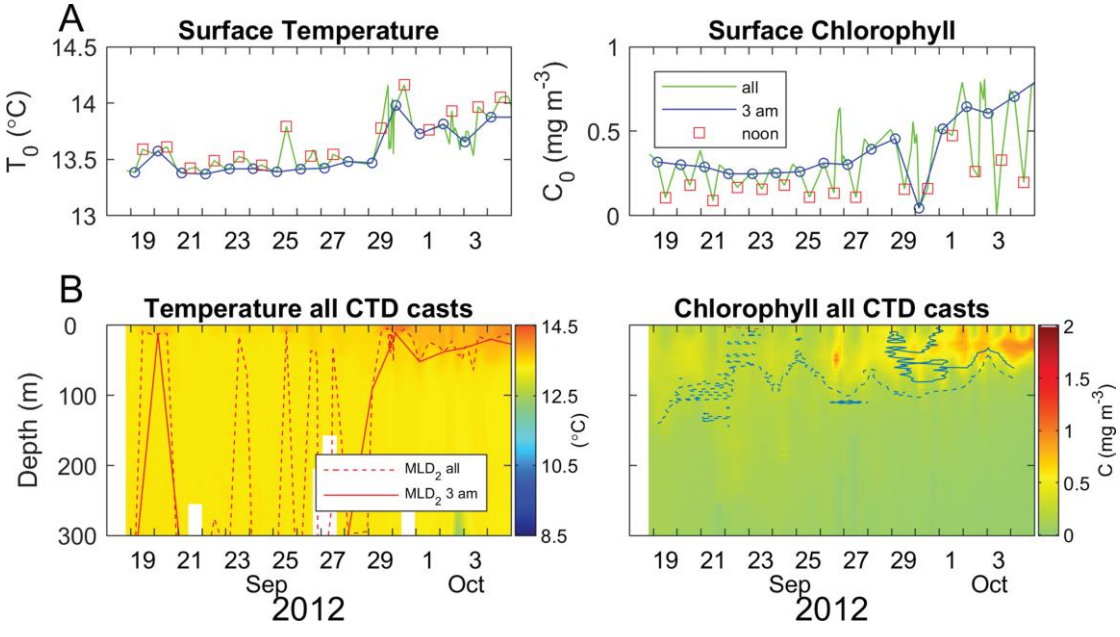
A
Surface Temperature
T0 (°C)
14.5
14
13.5
13
19 21 23 25 27 29 1 3
Surface Chlorophyll
C0 (mg m-3)
1
0.5
0
all
3 am
noon
19 21 23 25 27 29 1 3
B
Temperature all CTD casts
Depth (m)
0
100
200
300
MLD2 all
MLD2 3 am
14.5
12.5
10.5
8.5
(°C)
19 21 23 25 27 29 1 3
Sep
Oct
2012
Chlorophyll all CTD casts
2
1.5
1
0.5
0
C (mg m-3)
19 21 23 25 27 29 1 3
Sep
Oct
2012

861

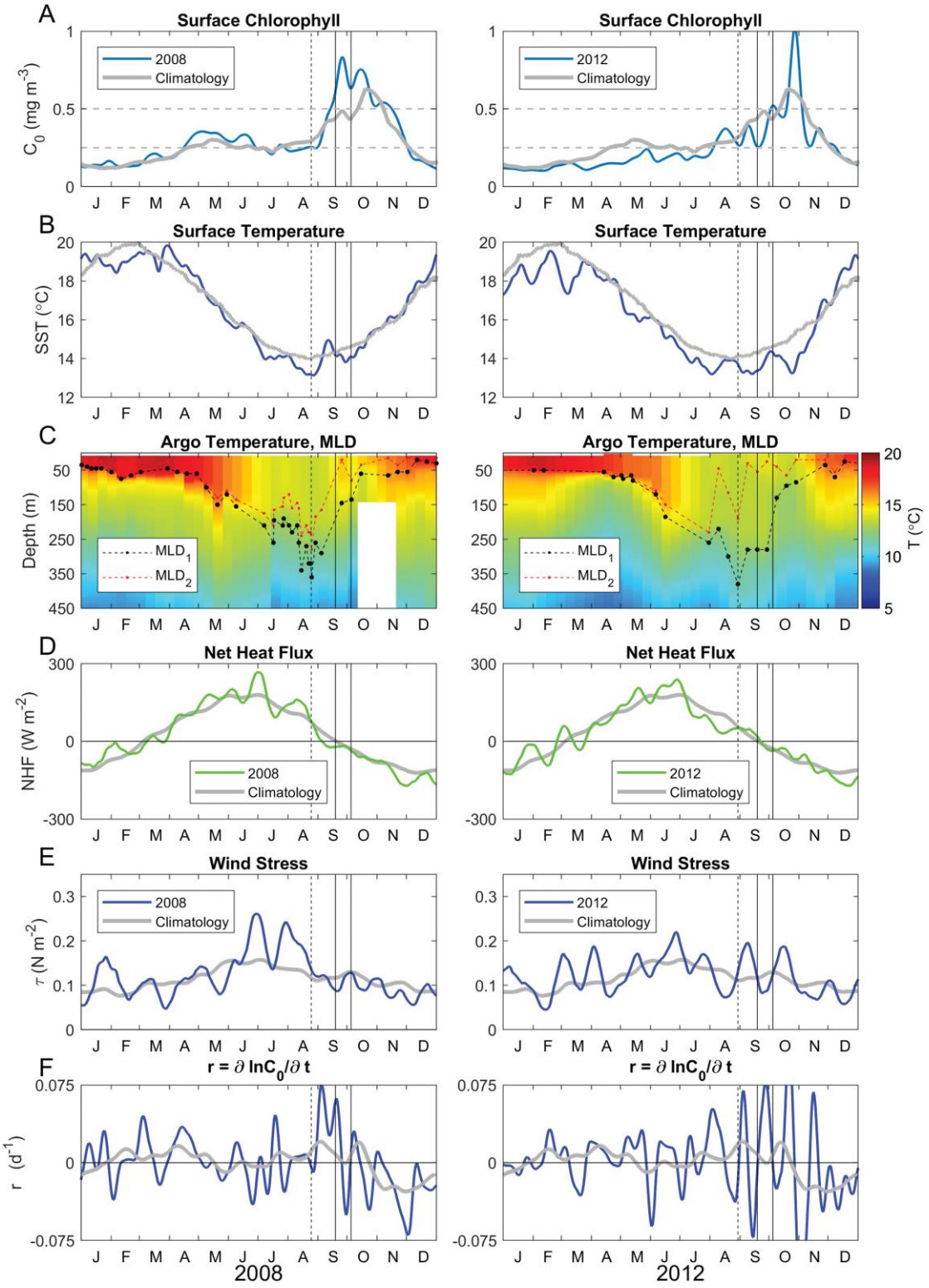
A
Surface Chlorophyll
2008
Climatology
C_0 (mg m^{-3})
Surface Chlorophyll
2012
Climatology
B
Surface Temperature
SST (°C)
Surface Temperature
C
Argo Temperature, MLD
Depth (m)
MLD$_1$
MLD$_2$
Argo Temperature, MLD
T (°C)
D
Net Heat Flux
NHF (W m^{-2})
2008
Climatology
Net Heat Flux
2012
Climatology
E
Wind Stress
τ (N m^{-2})
2008
Climatology
Wind Stress
2012
Climatology
F
r = ∂ lnC$_0$/∂ t
r (d^{-1})
r = ∂ lnC$_0$/∂ t
J F M A M J J A S O N D
2008
2012

862
863

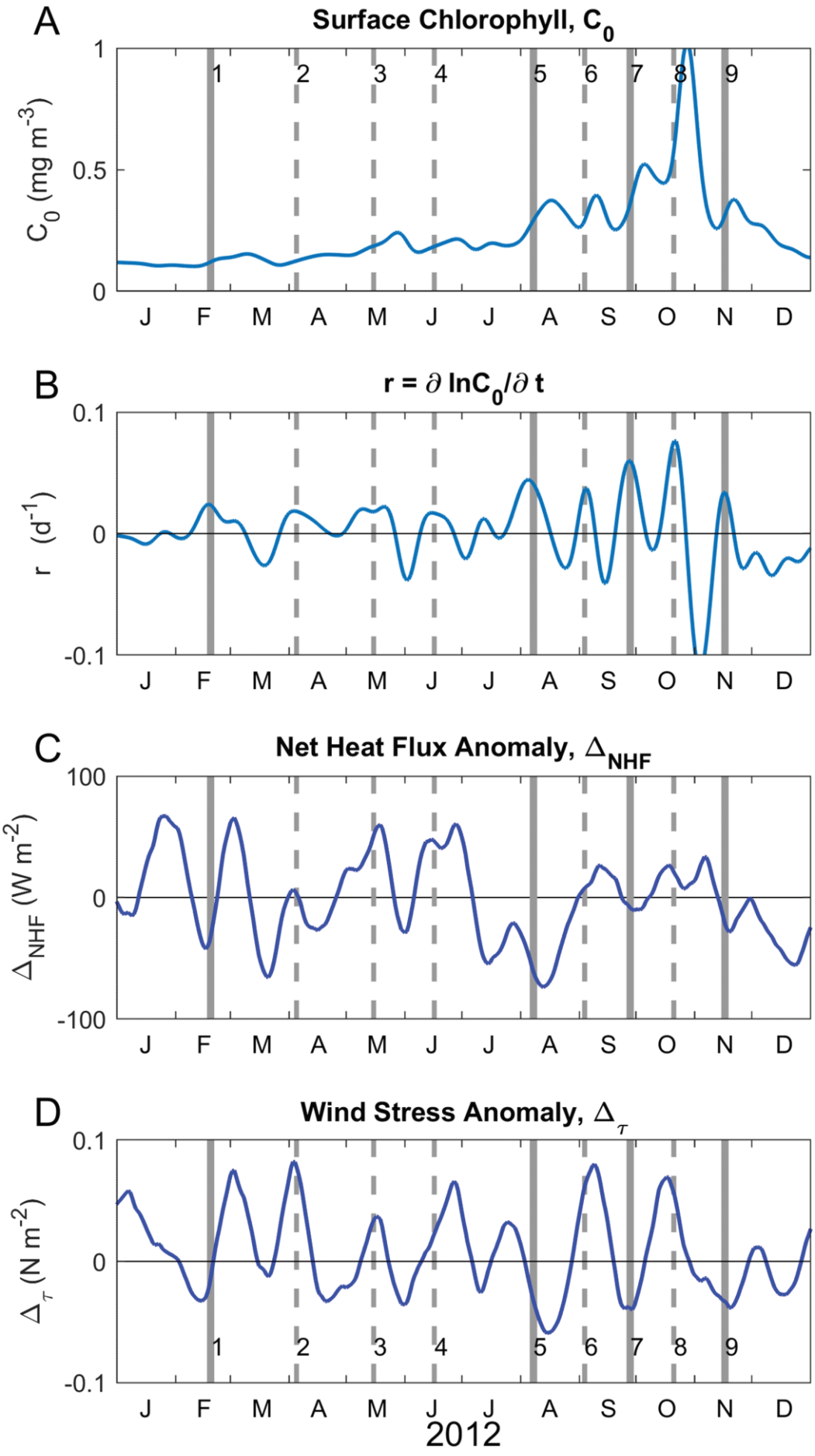
A
Surface Chlorophyll, C0
C0 (mg m-3)
1
0.5
0
1 2 3 4 5 6 7 8 9
J F M A M J J A S O N D
B
r = ∂ lnC0/∂ t
r (d-1)
0.1
0
-0.1
J F M A M J J A S O N D
C
Net Heat Flux Anomaly, ΔNHF
ΔNHF (W m-2)
100
0
-100
J F M A M J J A S O N D
D
Wind Stress Anomaly, Δτ
Δτ (N m-2)
0.1
0
-0.1
1 2 3 4 5 6 7 8 9
J F M A M J J A S O N D
2012

864

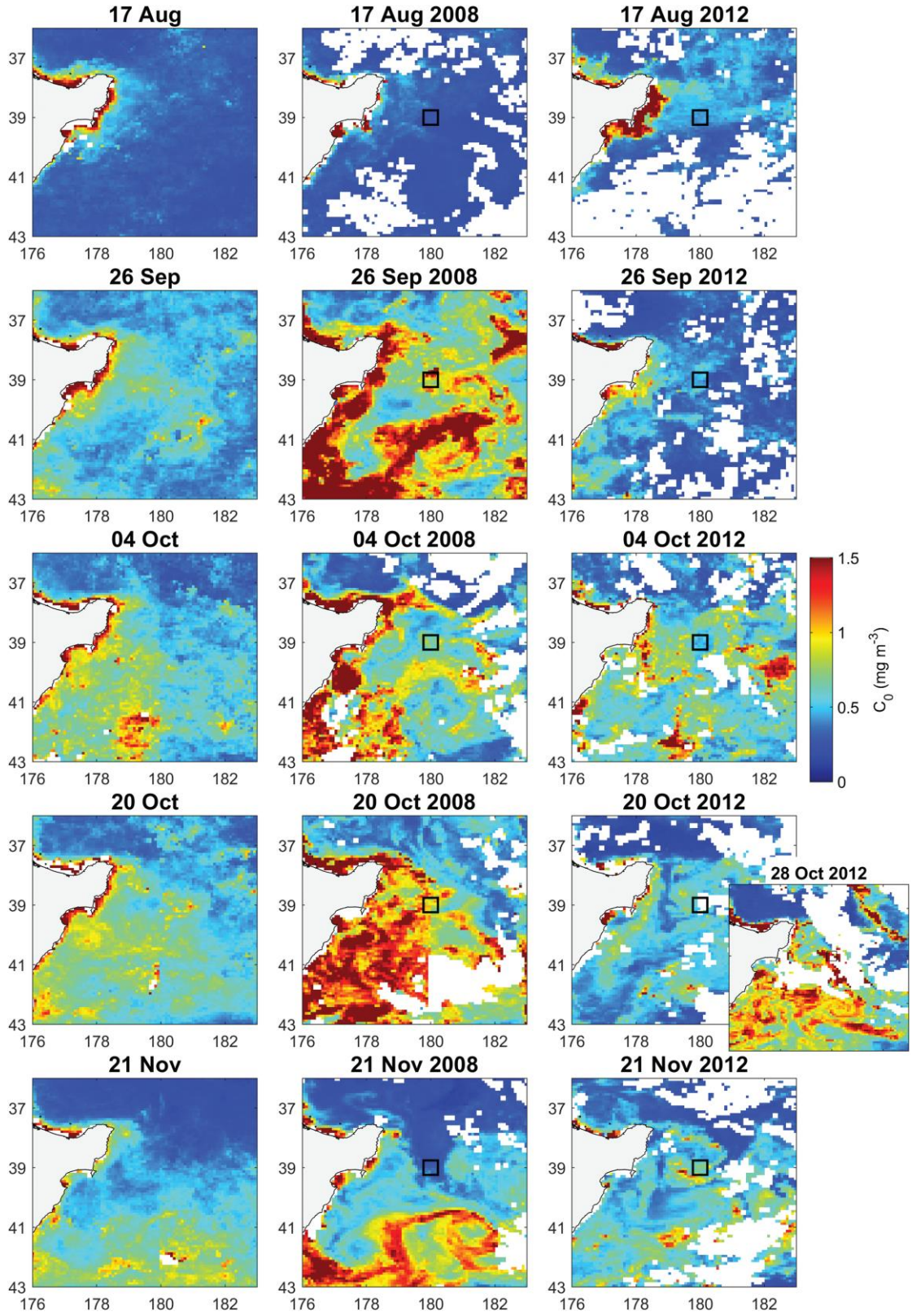
17 Aug
17 Aug 2008
17 Aug 2012
26 Sep
26 Sep 2008
26 Sep 2012
04 Oct
04 Oct 2008
04 Oct 2012
20 Oct
20 Oct 2008
20 Oct 2012
28 Oct 2012
21 Nov
21 Nov 2008
21 Nov 2012
37
39
41
43
176
178
180
182
1.5
1
0.5
0
C0 (mg m-3)

865
866

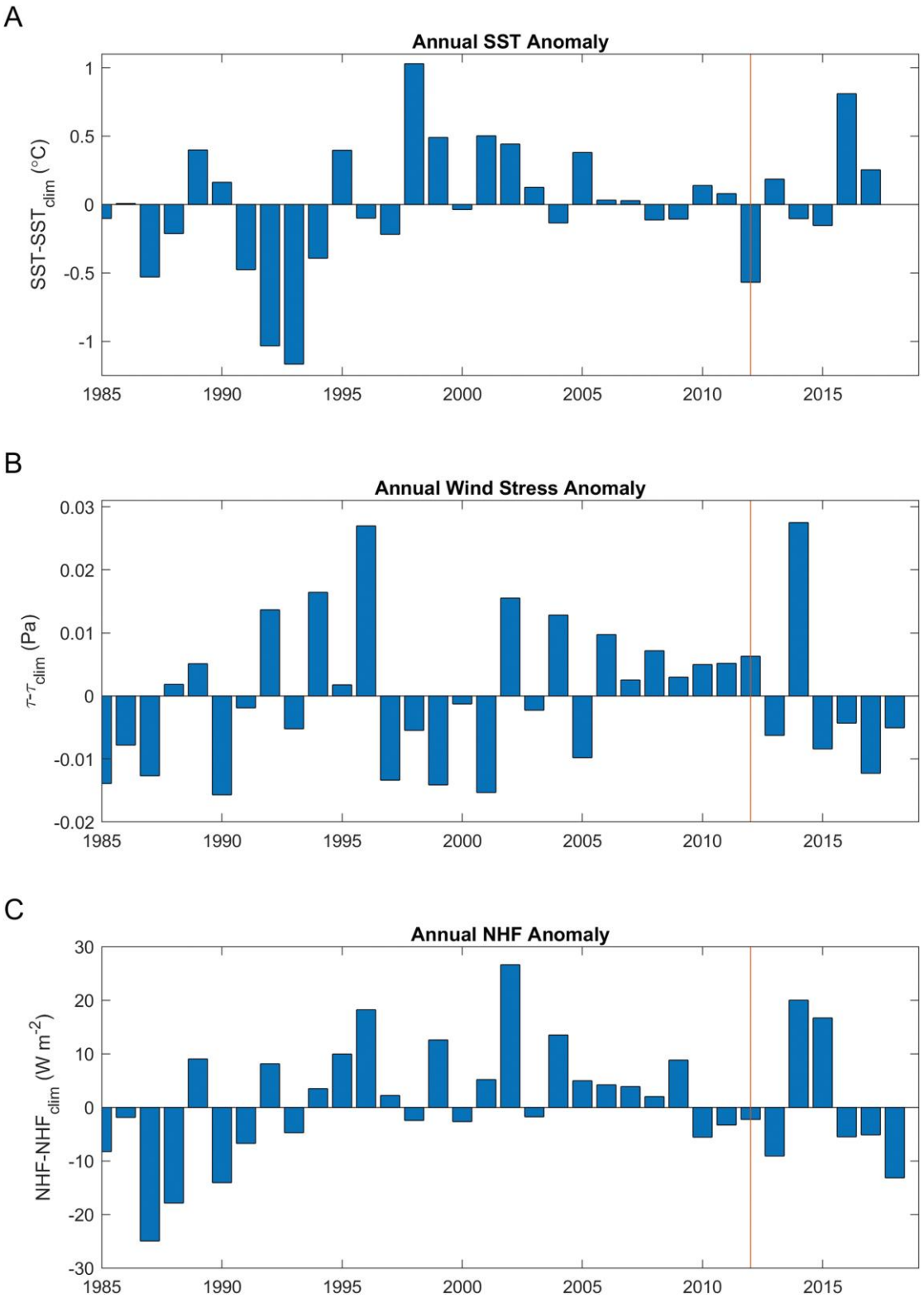
A
Annual SST Anomaly
SST-SST$_{clim}$ (°C)
1
0.5
0
-0.5
-1
1985
1990
1995
2000
2005
2010
2015
B
Annual Wind Stress Anomaly
τ-τ_{clim} (Pa)
0.03
0.02
0.01
0
-0.01
-0.02
1985
1990
1995
2000
2005
2010
2015
C
Annual NHF Anomaly
NHF-NHF$_{clim}$ (W m^{-2})
30
20
10
0
-10
-20
-30
1985
1990
1995
2000
2005
2010
2015

867
868
869